




Local production and imitations of Late Roman pottery from a well in the Roman necropolis of Cuma in Naples, Italy

Chiara Germinario¹ | Giuseppe Cultrone² | Laetitia Cavassa³ | Alberto De Bonis⁴ |
 Francesco Izzo¹ | Alessio Langella¹ | Mariano Mercurio¹ | Vincenzo Morra⁵ |
 Priscilla Munzi⁶ | Celestino Grifa¹ 

¹Dipartimento di Scienze e Tecnologie, Università del Sannio, Benevento, Italy

²Departamento de Mineralogía y Petrología, Universidad de Granada, Granada, Spain

³CNRS, Ministère de la Culture, Aix Marseille Université, Aix-en-Provence, France

⁴Institut für Klassische Archäologie, Universität Wien, Wien, Austria

⁵Dipartimento di Scienze della Terra, dell'Ambiente e delle Risorse, Università degli Studi di Napoli Federico II, Napoli, Italy

⁶Centre Jean Bérard, USR3133, CNRS-EFR, Napoli, Italy

Correspondence

Celestino Grifa, Dipartimento di Scienze e Tecnologie, Università del Sannio, Via Port'Arsa, 11, 82100 Benevento, Italy.
 Email: celestino.grifa@unisannio.it

Scientific editing by Noémi Müller

Funding information

LEGGE REGIONALE 5/02 ANNUALITA' 2008 Decreti Presidenziali, Grant/Award Numbers: 43 del 21.2.2011, 97 del 27.4.2011, 163 del 15.9.2010; Sannio University Research Fund; University Federico II of Naples Research Fund; Spanish Government, Grant/Award Number: MAT2016-75889-R

Abstract

Archaeological excavations performed in a funerary complex in Cuma (Campania region, Italy) unearthed excellently preserved common wares dated to the third century A.D. Archaeometric analyses were focused on Campanian pitchers, Aegean-like cooking pots, and pyriform pitchers, the latter recorded for the first time in an Italian context. The local pitchers were manufactured with a high-CaO clay (CaO = ca. 12 wt.%) and local volcanic temper, fired at ca. 800–850°C, as suggested by the presence of calcite. The Aegean-like pots and the pyriform pitchers were made with low-CaO clay (CaO ≤ 4.0 wt.%) mixed with a calcite-bearing temper, along with volcanic and siliciclastic grains, and fired at 800–950°C. The comparison with raw materials inferred that local vessels were made with low-CaO basinal clays which outcrop in the northern Campania region, and sands from the shoreline north of Cuma where carbonate, siliciclastic and volcanic phases mix together. Our results suggest that the Phlegraean Late Roman workshops produced their traditional vases along with imitations of Aegean-like pottery. Thus, microregional production responded to a market demand requiring shapes and styles similar to imports from the eastern Mediterranean, with which commercial trade was still quite active.

KEYWORDS

Aegean pottery imitations, calcite-bearing temper, ceramic technology, Cuma, Late Roman pottery

1 | INTRODUCTION

The ancient town of Cuma (Figure 1a) was founded in 740 B.C. and represents one of the oldest Greek settlements of the Western Mediterranean Sea. Its remains document ca. 20 centuries of human history and material culture, from its foundation to abandonment in the 13th century A.D. From a small pre-Hellenistic settlement, Cuma became an important Greek city during the last quarter of the eighth century B.C. The Samnites conquered the city in the second half of the fifth century B.C. and remained up until the second half of the fourth century B.C., when the Romans occupied the Campanian

coasts. During the sixth century A.D., Cuma was the battlefield of the Goths versus the Byzantines, and subsequently the town became a pirates' cove up until its final occupation by the Duchy of Naples in the 13th century (Brun & Munzi, 2011). Cuma's archaeological history began to be revealed in the 17th century, when archaeological surveys performed during the Bourbon period unearthed the remains of the ancient town (Brun & Munzi, 2010).

Today, Cuma is one of the most representative archaeological sites of the Campania region revealed in part due to three large research projects, Kyme I, II, and III, all of which have focused on preserving and promoting this important historical heritage of the

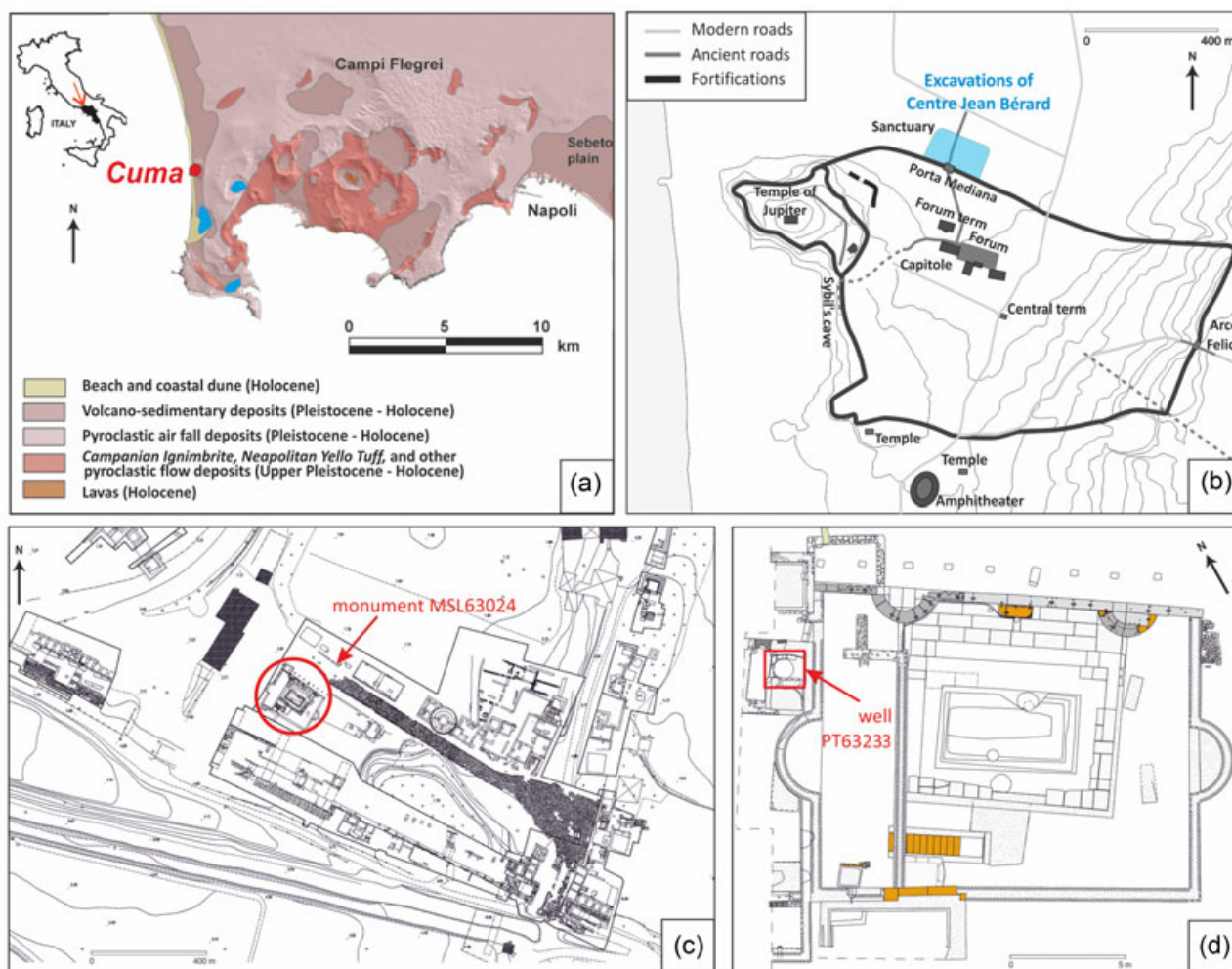


FIGURE 1 (a) Geological sketch map of Phlegraean area (modified by Izzo et al., 2016) with the location of Cuma; (b) site map of Cuma with the excavation area of the *Centre Jean Bérard* (contour interval = 25 m; modified by Cavassa et al., 2018); (c) scheme of the Roman necropolis where the Funerary Complex of the Sphinx (MSL63024) was discovered (contour interval = 0.5 m); (d) detailed scheme of the mausoleum in which the well (PT 63233) was found [Color figure can be viewed at wileyonlinelibrary.com]

Phlegraean area (Brun & Munzi, 2010). Within the Kyme projects, a large quantity of ceramic materials was collected. This collection became the object of a wide project of archaeometric characterization carried out by the *Centre Jean Bérard*, the University of Sannio, and the University “Federico II” of Naples, and represented an important opportunity for individuating the technological skills of local artisans, tracing commercial patterns, and depicting the socio-economic vitality of the town.

Archaeological and historical sources, largely supported by archaeometric data, addressed a long ceramic tradition spanning from the Archaic period up to the Byzantine, as also attested in other sites around the Bay of Naples (Olcese, 2010, 2012, 2017). This ceramic production encompassed various styles, typologies, and technologies, including common and fine wares (such as *Rosso Pompeiano* and Thin Walled pottery) as well as prototypes of modern technical ceramics (crucibles for pigment synthesis; Borriello, Giglio, & Iavarone, 2016; De Bonis et al., 2018; Greco et al., 2014; Grifa, Morra, Langella, & Munzi, 2009a; Guarino et al., 2011; Morra et al., 2013; Munzi et al., 2014). Hence, Cuma can be

considered among the major ceramic manufacturing centers of the Campania region. Moreover, due to the proximity of important ports and commercial hubs such as Puteoli and Misenum, local productions often existed alongside imported pottery (De Rossi, 2002; Piromallo, 2004).

The discovery of Late Roman pottery on the northeast side of Cuma in 2006 by archaeologists from the *Centre Jean Bérard* (Figure 1b) provided much needed data on the Late Roman Ceramics from Cuma, filling a gap in archaeometric studies that had been conducted up until that point. Here, a monumental Roman necropolis superimposed on sanctuary and funerary structures from the Iron Age to the Greek period was unearthed (Brun & Munzi, 2010). The Roman necropolis, dating from the second century B.C. to the sixth century A.D., consisted of numerous mausoleums, tombs, and isolated funerary enclosures (Brun & Munzi, 2010), including the monumental Funerary Complex of the Sphinx (Figure 1c,d). The western part of the funerary complex was transformed into a workshop during the Late Roman period (unfortunately what was produced is still unknown), as highlighted by a well for water supply (Figure 1d) and two basins. The well represented a unique

closed context that preserved several ceramic artifacts of the third century A.D. with an exceptional state of preservation and representativeness. Most of the vessels were intact, and pertained to both local and imported productions, as suggested by both their stylistic and typological features (Cavassa et al., 2018).

The locally manufactured pottery mostly consisted of pitchers widely produced during the Late Roman period in Campania, whereas the imported pieces displayed stylistic similarities with African and Aegean vessels (Cavassa et al., 2018). In particular, the occurrence of the so-called corrugated cooking pots drew the attention of the archaeologists due to their morphological consistency with artifacts produced in Eastern Mediterranean sites (Istenič & Schneider, 2000 and reference therein). Indeed, the main production centers of such vessels were in Western Asia Minor, in the ancient region of Phocaea, Attica, and the Aegean islands (Istenič & Schneider, 2000), from which they were widely exported along the entire Mediterranean coast, as confirmed by discoveries in Adriatic sites, Northwest Africa, the south of France, and western Italy (Albarella, Ceglia, & Roberts, 1993; Ceazzi & Del Brusco, 2014; Gliozzo, Fortina, Turbanti, Turchiano, & Volpe, 2005a; Istenič & Schneider, 2000). The widespread diffusion of these styles documents a massive production that began to be imitated in southern Italy during the Late Roman period when commercial trading in the Mediterranean abruptly declined, thus catalyzing the diffusion of microregional workshops in response to the disappearance of a large scale production (Arthur, 2007).

This paper provides the results of mineralogical, petrographic, and chemical analyses of the most representative vessels collected from the well of the Funerary Complex of the Sphinx, with the aim of identifying key elements useful for inferring provenance, technology, and post-depositional alteration and contamination. Particular attention was focused on the Aegean-like pottery due to its diffusion in Late Roman commercial trade throughout the Mediterranean. Was this pottery locally produced imitation pottery or imported? If the pottery was imported, which route to Cuma did the vessels follow? If local artisans produced imitation pottery, why did they choose to imitate such vessels? The response to these questions could open up interesting scenarios in terms of the circulation of pottery (and goods) during the Late Roman period, generally characterized as a period of profound crisis. With regard to the (presumed) local production, the reconstruction of the technologies utilized could provide further information on Campanian Late Roman pottery.

The case of Cuma reported herein is set within a wider investigation of Late Roman Campanian pottery focused on characterizing different microregional key districts, to better outline the economy, commercial trade, and technologies used during the Late Roman period (Germinario, 2015; Germinario et al., 2018).

2 | ARCHAEOLOGICAL CONTEXT

Archaeological surveys performed in the northern part of ancient Cuma (Figure 1b) suggest that this area had served both as a funeral space and sanctuary since the Archaic period. Only from the Late

Republican period (second century B.C.) did it assume a solely funerary function up to the Late Roman period (the second half of fourth century A.D.).

Here, the Funerary Complex of the Sphinx (monument MSL63024) located west of Porta Mediana is the most outstanding and tangible structure of the site (Figure 1c). This monumental tomb experienced at least four building phases: (a) The construction of the mausoleum enclosure and monumental façade along with the tuff basement, dated to the Augustan-Tiberian age; (b) the raising of the floors due to a rise in groundwater during the first century; (c) a partial obliteration of the mausoleum during *Domitian* road construction, and finally, (d) new building interventions affecting the western side of the monument and other neighboring tombs and the installation of a new artisanal workshop in this area during the third century A.D. The funeral complex was abandoned during the last decade of the third century due to a natural disaster (probably an earthquake) as demonstrated by a small treasure of 63 *antoniniani* dating back to A.D. 270–271. Lastly, during the second half of the sixth century A.D., the necropolis was used as a quarry for limestones and marbles for lime production (Brun & Munzi, 2011; Brun & Munzi, 2010; Brun, Munzi, & Botte, 2018).

Our research focused on the fourth building phase related to the artisanal workshop, which exploited water from three basins and a 4.5-m-deep well with a reservoir chamber (Figure 1d). Archaeological surveys in the well permitted the collection of 70 ceramic artifacts, along with some metal objects (lead and iron), one glass plate, and animal remains. The vessels displayed an exceptional state of preservation, permitting a restoration to their original form. The state of preservation and the typological *repertoire* (see hereafter) indicated that the well was not a dump. The vessels were most probably lost during water collection up until the well was abandoned and later sealed for safety reasons, probably due to the fact that animal carcasses were thrown in it. Almost all the unearthed ceramic items preserved a handle, corroborating further the theory that the well was utilized for water collection.

3 | POTTERY AND SAMPLING STRATEGY

Seventy items were unearthed in the well including 59 common wares, six amphorae, three lamps, and two fine wares (Cavassa et al., 2018). Our analysis focused on the common wares, the most representative and interesting class from an archaeological point of view, divided into various forms of table and cooking wares (see Figure 2). The tableware (48 items; 81.4% of the assemblage) included 23 pyriform pitchers, 14 painted pitchers, eight continuous profile pitchers, and three bottles (Cavassa et al., 2018; Figure 2). The cooking ware was represented by eight pots, one kettle, and two lids, representing ca. 18.6% of the total sample.

The sampling strategy adopted for the archaeometric analysis was guided by three different purposes: (a) Typological representativeness

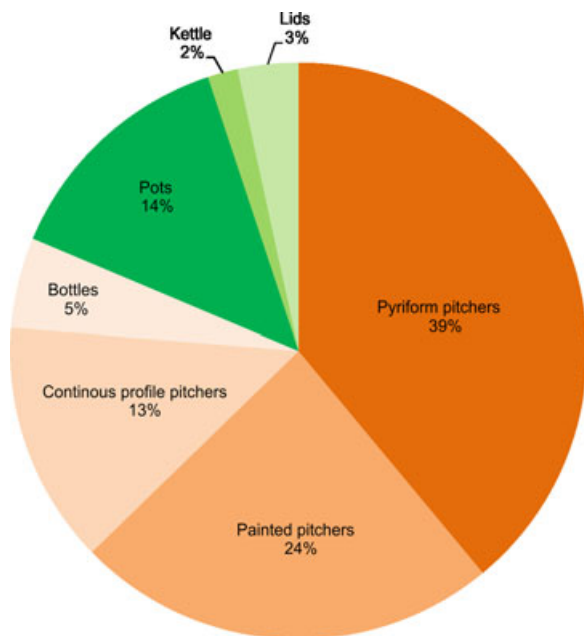


FIGURE 2 Percentages of common wares recovered in well PT 63233 ($n = 59$ items) [Color figure can be viewed at wileyonlinelibrary.com]

in the archaeological records; (b) samples of common ware with clues (form, fabric) of importation; and (c) samples of common ware having clues (form, fabric) of local production. Twelve vessels were selected, namely, seven samples of the pyriform pitchers, two samples of the painted pitchers, two cooking pots, and one kettle (Table 1). Their typological features and fabric description are reported below.

The pyriform pitchers (CM 15, 16, 17, 18, 22, 25, 27) show small single-rounded or pronounced rims (Figure 3; samples CM 15, 16, 25, 27), a narrow base with a characteristic convex foot and a vertical handle with an oval section (Cavassa et al., 2018). The ceramic bodies are medium-textured with hard or very hard pastes, and in some

cases the clay body is zoned (Table 1). To date, such an assemblage of pitchers with the same typological and stylistic features has not been found in any other Italian archaeological context, except for one ceramic piece recovered in Pozzuoli, dating to the third century A.D. (Orlando, 2014). In contrast, the painted pitchers (CM 19, 24) are characterized by a large body, marked by vertical stripes, a ring foot, and a vertical handle, with the upper part covered with a thin slip applied by immersion (Figure 3; samples CM 19, 24; Cavassa et al., 2018). Morphological similarities with the pitchers found at the Imperial villa of Somma Vesuviana (Mukay & Aoyagi, 2014) suggest that they belong to a third century A.D. regional (local) production. Macroscopic features of the ceramic body highlighted a fine- or medium-textured paste, yellowish red or brown in color, and on some occasions zoned (Table 1).

With regard to the cooking ware, the pots (Hayes 2 form; CM 09, 20), traditionally called “corrugated cooking pots,” are of Aegean tradition (Figure 3; samples CM 09, 20), whereas the full profile kettle (CM 21) has a trilobate rim and vertical handle bottom (Figure 3; sample CM 21). The ceramic bodies are hard or very hard medium- or fine-textured pastes; the colors range from brown or dark yellowish for the two pots, whereas the kettle showed a zoned matrix, with a red core and dark brown rims (Table 1). A striking feature of the corrugated cooking pots, is the occurrence of “calcite-spots” in their fabrics, which seems to be a common element with the pyriform pitchers discovered in the well (Cavassa et al., 2018).

4 | BRIEF GEOLOGICAL REMARKS

Cuma is located in the Phlegraean Fields volcanic district, a complex caldera system situated west of the city of Naples and south of the mouth of the Volturno River (Figure 1a). Quaternary volcanic activity, essentially consisting of large explosive eruptions mainly due to water/magma interactions, caused the formation of polygenic calderas in

TABLE 1 Archaeological information and macroscopic features of analyzed cooking ware and table ware

Ceramic class	Sample	Shape	Type	Dating	Colour			Hardness	Texture
					Core	Rims	Zoning		
CW	CM 09	Pot	Hayes 2	First half third century A.D.	7.5YR 4/3	7.5YR 4/3	-	Hard	M, R, Abb
	CM 20	Pot	Hayes 2	First half third century A.D.	10YR 4/4	10YR 4/4	-	Very hard	F, R, Mod
	CM 21	Kettle	-	First half third century A.D.	2.5YR 4/6	7.5YR 3/2	Sharp	Hard	F, R, Mod
TW	CM 15	Pitcher	-	First half third century A.D.	7.5YR 3/2	5YR 5/6	Faded	Hard	F, R, Abb
	CM 16	Pitcher	-	First half third century A.D.	10YR 4/4	10YR 4/4	-	Hard	M, R, Mod
	CM 17	Pitcher	-	First half third century A.D.	2.5YR 5/8	2.5YR 5/8	-	Very hard	F, R, Sp
	CM 18	Pitcher	-	First half third century A.D.	2.5YR 5/8	7.5YR 4/6	Sharp	Hard	F, R, Mod
	CM 19	Painted pitcher	-	First half third century A.D.	5YR 5/8	10YR 4/6	Faded	Hard	M, R, Mod
	CM 22	Pitcher	-	First half third century A.D.	2.5YR 5/6	2.5YR 5/6	-	Hard	F, R, Mod
	CM 24	Painted pitcher	-	First half third century A.D.	7.5YR 5/4	7.5YR 5/4	-	Very hard	F, R, Sp
	CM 25	Pitcher	-	First half third century A.D.	5YR 5/6	5YR 5/6	-	Hard	F, R, Sp
	CM 27	Pitcher	-	First half third century A.D.	7.5YR 5/4	7.5YR 5/4	-	Very hard	F, R, Mod

Note. Color code from Munsell Soil Color Chart.

Abbreviation of textural parameters from Williams (1990): Ab: abundant frequency of grains; CW: cooking ware; F: fine grain size (<0.25 mm); M: medium grain size (0.25–0.5 mm); Mod: moderate frequency of grains; R: rounded grains; Sp: sparse frequency of grains; TW: table ware.

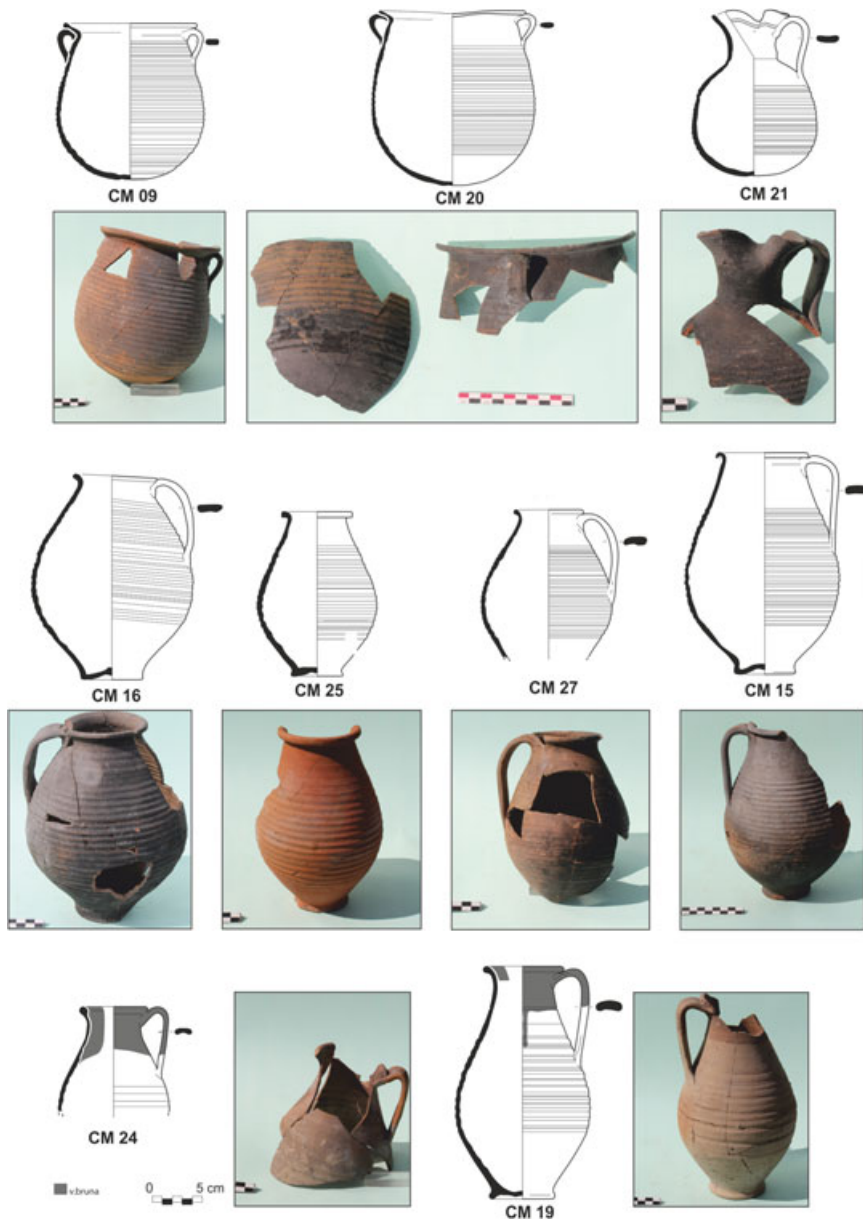


FIGURE 3 Ceramic finds and forms of pottery in well PT 63233. CM 09, CM 16: corrugated cooking pots; CM 21, kettle; CM 15, 16, 25, 27: pyriform pitchers; CM 19, 24: painted pitchers [Color figure can be viewed at wileyonlinelibrary.com]

which lower explosive eruptions produced monogenetic pyroclastic vents up until the last eruption of Mt. Nuovo in A.D. 1538 (Barberi et al., 1978; Morra et al., 2010; Orsi, De Vita, & di Vito, 1996; Rosi, Sbrana, & Principe, 1983). The 39 ka Campanian Ignimbrite (CI; Fedele et al., 2008; Langella et al., 2013) and 15 ka Neapolitan Yellow Tuff (NYT; Deino, Orsi, De Vita, & Piochi, 2004) represented the most intense Phlegraean eruptions, emplacing huge volumes of pyroclastic rocks that have been used as stratigraphic markers for the reconstruction of Phlegraean volcanic history and recognition of two main periods: precalderic and postcalderic (Orsi et al., 1996; Rosi et al., 1983). During the precalderic period, namely before the CI eruption, volcanic activity was mainly submarine, with lower subaerial episodes, principally emplacing lava domes. Today, the city of Cuma lies on a lava dome (Grifa et al., 2009a). The CI eruption left a large caldera depression, later invaded by the sea. The submarine activity continued during the

postcalderic period, up until the phreatoplinian eruption of NYT, which caused another caldera collapse within the previously formed CI caldera (Deino et al., 2004). The recent volcanic activity took place in the NYT caldera and on its margins, mainly forming tuff rings and tuff cones, suggesting that the eruptions were mostly triggered by water/magma interactions (Orsi et al., 1996).

Volcanic rocks of the Phlegraean Volcanic District vary in composition from shoshonitic basalts to trachytes and trachyphonolites, belonging to the shoshonitic series (Fedele et al., 2008). Pyroclastic rocks largely prevail and are composed of trachytes and trachyphonolites, including the CI and NYT deposits. The volcanic rocks contain K- to Na-rich sanidine, Na-plagioclase, Fe-rich clinopyroxene, and Fe-rich amphibole with accessory apatite, zircon, titanite, nepheline, and sodalite. Biotite and magnetite also occur in latites, whereas olivine is present in the least evolved lithotypes (Morra et al., 2013).

With respect to sources of clay, basinal sediments along with alluvial deposits and strongly weathered pyroclastic soils are exposed in the study area and farther inland (De Bonis et al., 2013). Basinal clays mainly crop out along the Apennine chain and are composed of clayey deposits of the lower Messinian Sicilide Unit (*Argille Varicolori*) and by the Mio-Pliocene successions of the Pietraraja Formation (Bonardi, Ciarcià, Di Nocera, Montano, & Sgrosso, 2009). Upper Pleistocene marine clays are exposed on the island of Ischia, considered to be one of the most important clay sources in the Bay of Naples (De Bonis et al., 2013; Grifa et al., 2009a). Alluvial clayey sediments are mostly represented by Quaternary river deposits that fill the flood plains of the Volturno River. Clays derived from weathered pyroclastic deposits are locally exposed around the Campanian volcanoes (the Phlegraean Fields, Somma-Vesuvius, and Roccamonfina) and, in some cases (e.g., the village of Cascano near Roccamonfina and Sorrento Peninsula), are currently used for traditional ceramic production (De Bonis et al., 2013).

5 | ANALYTICAL METHODS

Chemical, mineralogical, and petrographic analyses permitted an in-depth archaeometric characterization; the analytical strategy was spurred by the availability of archaeological materials (considering that most of the pieces were intact) and the representativeness of the samples in their typological group. Petrographic and textural features of ceramic pastes were investigated by means of polarized light microscopy in thin sections, using a Nikon Eclipse 6400 POL (Nikon Corporation, Tokyo, Japan) microscope. On a collage of photomicrographs, image analysis was performed using the ImageJ software package (National Institutes of Health, Bethesda, MD). Grain size distribution (GSD) was evaluated considering the minimum Feret (mF) value, used to calculate Krumbein ϕ ($\phi_{mF} = -\log_2(mF)$), whereas the circularity value ($C = 4\pi(A/p^2)$, where A = area, p = perimeter) was considered to be a shape descriptor. Density histograms were constructed using R software (R Development Core Team, 2008).

Chemical composition, in terms of major oxides (SiO₂, TiO₂, Al₂O₃, Fe₂O₃, MnO, MgO, CaO, Na₂O, K₂O, P₂O₅ in wt.%) and trace elements (Rb, Sr, Y, Zr, Nb, Ba, Cr, Ni, Sc in parts per million [ppm]), was obtained by means of an X-ray fluorescence (XRF) AXIOS PANalytical Instrument (Malvern Panalytical Ltd., Marvel, UK). The XRF data were treated by a statistical multivariate approach, which permitted an evaluation of the chemical behavior of the ceramic fragments in a multidimensional space, using R software (Bell Laboratories, Murray Hill, NJ). Raw chemical data were standardized by a log₁₀ transformation to avoid the risk of a false classification of objects with input variables with very different variances, as in the case of chemical concentrations (De Bonis et al., 2016; Grifa et al., 2009a); moreover, chemical elements easily influenced by burial conditions (MnO, P₂O₅, Ba) were omitted (Fabbri, Guarini, Arduino, & Coghé, 1994; Maggetti, 2001).

The statistical procedure was carried out utilizing R software (R Development Core Team, 2008), as described by Grifa, Morra, Langella, Cultrone, & Sebastián (2006), Grifa et al. (2009a,b), Grifa et al. (2013), and De Bonis et al. (2016). The principal component analysis

(PCA) resulted in ca. 90% of cumulative variance at the 11th component. The variables affecting the first 11 components were as follows: TiO₂, Al₂O₃, Fe₂O₃, MgO, Na₂O, K₂O, Rb, Y, Zr, Nb, and Ni. Subsequently, hierarchical clustering analysis (HCA) on the matrix of the distance was applied on the data set reduced by the PCA, permitting the clustering of the samples in a dendrogram using an agglomerative clustering algorithm.

Semiquantitative mineralogical analysis was carried out by means of X-ray powder diffraction (XRPD) using a PANalytical X'Pert PRO 3040/60 PW diffractometer (CuK α radiation, 40 kV, 40 mA, scanning interval 4–50° 2 θ , equivalent step size 0.017° 2 θ , equivalent counting time 15.5 s per step, RTMS X'Celerator detector), equipped with X-Pert data collector software and X-Pert High Score Plus for data analysis (Malvern Panalytical Ltd., Marvel, UK). The ceramic samples were first finely powdered (grain size < 10 μ m) with a McCrone Micronizing Mill (The McCrone Group, Inc., Westmont, IL) (agate cylinders and wet grinding time 15 min) to avoid a preferred orientation and an α -Al₂O₃ internal standard (1 μ m, Buehler Micropolish) was added to each sample (20 wt.%) to perform quantitative analyses (Bish & Reynolds, 1989), which are not reported in this paper.

Thermogravimetric (TG) and differential scanning calorimetric analyses with simultaneous Fourier transform infrared (FTIR) spectroscopy for evolved gas analysis (EGA) were performed using a Netzsch STA 449 F3 Jupiter thermal analyzer (NETZSCH Group, Selb, Germany) coupled with a Bruker Tensor 27 (Bruker, Billerica, MA). Powdered samples (20–30 mg) were placed in alumina crucibles and heated from room temperature up to 1150°C at 10°C/min of heating rate in an ultrapure air-purged, silicon carbide furnace. The FTIR spectra were acquired using 8 cm⁻¹ resolution, 32 spectra scans per minute, and 100 spectra scans for background. Netzsch Proteus 6.1.0 and Opus 7.0 software were used for data analysis. Thermal analyses, as well as XRPD analysis, were performed on all the samples, except for CM 15, CM 22, and CM 24, due to the small amount of material available.

Scanning electron microscopy/energy-dispersive X-ray spectroscopy (SEM/EDS) microanalyses on carbon-coated and polished thin sections were performed by means of a SEM Zeiss EVO HD15 (Carl Zeiss, Oberkochen, Germany), operating at 20 kV accelerating voltage, 200 pA I probe current and spot size of 429 μ m, equipped with an Oxford Instruments Microanalysis Unit (Xmax 80 EDS detector). The Smithsonian Microbeam Standards (Carpenter, Counce, Kluk, & Nabelek, 2002; Donovan et al., 2002, 2003; Jarosewich, 2002; Jarosewich & Boatner, 1991; Jarosewich & MacIntyre, 1983; Jarosewich & White, 1987; Jarosewich, Gooley, & Husler, 1987; Vicenzi, Eggins, Logan, & Wysoczanski, 2002) were used for EDS calibration.

6 | RESULTS AND DISCUSSION

6.1 | Petrography, mineral chemistry and chemical composition of the ceramic bodies

With regard to the potsherds, all samples were generally characterized by fine to coarse-grained pastes, in which the temper grains were deliberately added, as observed in the skewed GSD curves showing a negative tail toward the coarser particles (Figure 4). In

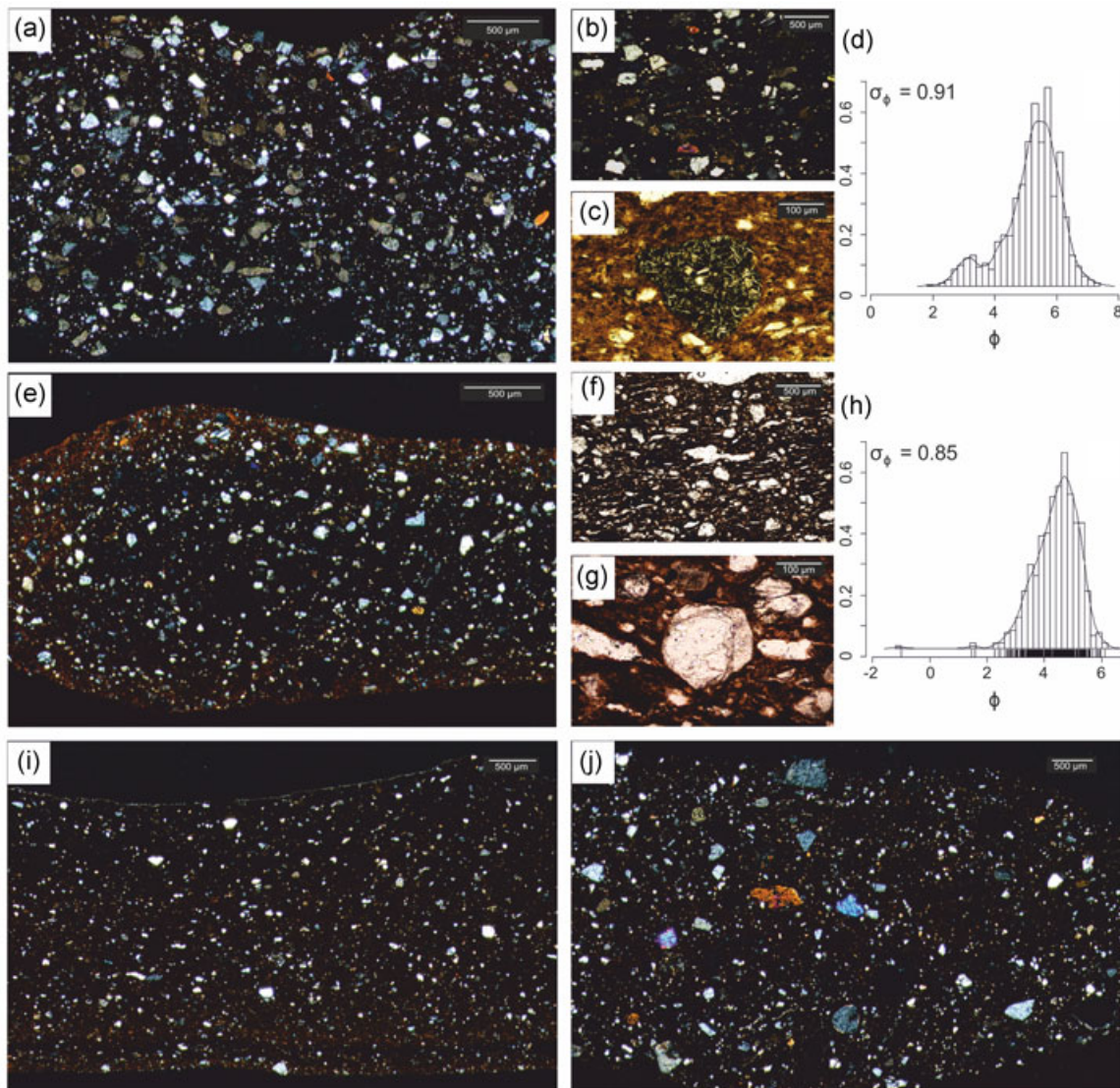


FIGURE 4 Photomicrographs of analyzed samples and density histograms of GSD. (a) Group 1, ceramic body, sample CM 9, crossed polars; (b) Group 1, temper grains, sample CM 16, crossed polars, $\times 40$; (c) Group 1, volcanic scoria, sample CM 22, plane polarized light, $\times 100$; (d) Group 1, GSD, sample CM 9; (e) Group 2, ceramic body, sample CM 25, plane polarized light; (f) Group 2, siliciclastic temper, sample CM 21, plane polarized light, $\times 40$; (g) Group 2, leucite crystal, sample CM 25, plane polarized light, $\times 200$; (h) Group 2, GSD, sample CM 25; (i) Sample CM 24, seriate texture, crossed polars; (j) Sample CM 19, ceramic body, crossed polars. GSD: grain size distribution [Color figure can be viewed at wileyonlinelibrary.com]

contrast, the mineralogy of the temper grains distinguished two different groups, including both table and cooking ware, and two loners. In fact, both the textures and mineralogy of the ceramic body are not associated with the typological features of the pottery, namely the table or cooking ware. In particular, the mineralogical criterion for discriminating the groups was the abundance of calcite grains among the temper particles.

Group 1 was composed of the pot CM 09 and the pyriform pitchers CM 15, CM 16, CM 22 and CM 27 (Table 2; Figure 4a). The temper grains were mainly constituted by calcite grains with lower siliciclastic (Figure 4b) and volcanic phases (Figure 4c) scattered in light brown to brown isotropic or red anisotropic matrices along with finer crystals of quartz, feldspar, and rare mica, representing the residual aplastic particles that occurred in the clayey deposits. The

aplastic grains were arranged in a bimodal texture, as highlighted by the skewed ϕ size curves on the GSD histograms (Figure 4d). They can be considered a further proof of the temper addition, along with the mineralogical difference between coarser (carbonatic + volcanic + siliciclastic) and finer fractions (siliciclastic). The particles generally presented a subcircular shape (average $C = 0.80$), varying in the GSD from fine silt (0.01 mm) to coarse sand (0.55 mm) with subordinate very coarse sand (up to 2 mm; Table 2; average $\phi_{mF} = 4.8$); the grain particles were moderately sorted (average $\sigma\phi = 0.85$) (Table 2). The calcite-bearing temper appeared partially or totally decomposed. The SEM observations showed that the decomposition process mainly affected the grain rims (Figure 5a) and only subordinately the entire grains, causing the formation of “ghosts” that maintained the shape of the original particles (Figure 5b). In the innermost part of the grains,

TABLE 2 Mineralogical and textural features of ceramic pastes, determined by polarized light microscopy and image analysis

Matrix		Color														Average C				
Sample	Core	Rim	Activity	Texture	Packing	Qz	Fsp	Mica	Cpx	Drf	Sc	Cb	Vgf	Amp	Garn	Ol	Lct	Average ϕ	σ_ϕ	Average C
Group 1	CM 09	Light brown	Isotropic	Bimodal	20–30%	xxxx	xxx	tr	tr	tr	tr	xxx	-	tr	-	tr	-	5.2	0.91	0.80
	CM 15	Red	Anisotropic	Bimodal	15–25%	xxx	xxx	tr	x	x	x	x	tr	tr	-	-	-	4.4	0.81	0.79
	CM 16	Dark brown	Isotropic	Bimodal	20–30%	xxxx	xxx	tr	tr	tr	tr	xxx	-	tr	-	-	-	4.3	0.92	0.81
	CM 22	Light brown	Anisotropic	Bimodal	10–20%	xxxx	xx	tr	tr	tr	tr	x	-	tr	-	-	-	4.9	0.72	0.80
	CM 27	Light brown	Anisotropic	Bimodal	10–20%	xxxx	xxx	tr	tr	tr	tr	x	xx	-	-	-	-	5.0	0.89	0.80
Group 2	CM 17	Red	Anisotropic	Bimodal	15–20%	xxx	xx	-	tr	tr	x	tr	-	-	-	-	-	5.0	0.77	0.80
	CM 18	Brown	Anisotropic	Bimodal	15–20%	xx	xx	-	tr	tr	x	tr	-	-	-	-	-	4.9	0.71	0.81
	CM 20	Light brown	Anisotropic	Seriate	10–15%	xxx	x	-	-	-	-	tr	-	-	-	-	-	5.4	0.68	0.79
	CM 21	Reddish brown	Isotropic	Bimodal	15–25%	xxx	xx	-	tr	tr	x	-	-	-	tr	-	-	4.7	0.74	0.82
	CM 25	Reddish brown	Anisotropic	Bimodal	15–25%	xxx	xxx	-	x	x	xx	-	tr	tr	-	-	tr	4.4	0.79	0.85
	CM 19	Red	Anisotropic	Bimodal	15–25%	xxxx	xxx	tr	x	xx	x	x	-	-	-	-	tr	5.0	0.81	0.80
	CM 24	Brown	Anisotropic	Seriate	5–10%	xxx	xx	tr	-	-	tr	-	-	-	-	-	-	5.3	0.60	0.82

Abbreviations (Whitney & Evans, 2010): Amp: amphibole; C: circularity; Cb: carbonate mineral; Cpx: clinopyroxene; Drf: Detrital rock fragments; Fsp: feldspar; Garn: garnet; Lc: leucite; Ol: olivine; Qz: quartz; Sc: scoriae; Tr: traces; Vgf: volcanic glass fragments; ϕ : grain size; σ : standard deviation.

well-preserved calcite crystals were occasionally observed along with fluorite (Figure 5c).

BSE images permitted the identification of a complex reaction rim (2–5 μm), developed at the interface between the calcareous particles and the clayey matrix (Figure 5d). The reaction rim was composed of CaO-depleted and $\text{SiO}_2\text{-Al}_2\text{O}_3$ -enriched dark gray areas, followed by a brighter contact with the clayey matrix, yielding the composition of an Al-rich clinopyroxene (Figure 5d). This complex chemically zoned rim marked the migration of CaO from calcite toward the Al_2O_3 and SiO_2 -rich clayey matrix interface, thus allowing the formation of Ca-silicates (Cultrone, Rodriguez-Navarro, Sebastian, Cazalla, & De La Torre, 2001; Rathossi & Pontikes, 2010).

Along with the carbonate temper, minor mixed siliciclastic and volcanic phases were also added to the ceramic pastes. Quartz, alkali feldspar, plagioclase, along with a lower amount of clinopyroxene, micas, amphiboles, scoriae (Figure 4c), volcanic glass and arenaceous fragments, were observed. The quartz showed a nearly pure SiO_2 composition, whereas the crystals of feldspar were mainly constituted by K-feldspar ($\text{An}_0\text{Ab}_{2-24}\text{Or}_{98-76}$), occasionally containing barium oxide up to 1.8 wt.%, and fewer plagioclase (Supporting Information Figure 1a). EDS microchemical analyses (Supporting Information Table 2) of colorless diopside evidenced a FeO concentration of 6.4 and 11.2 wt.% for a pale green Fe-rich diopside (Supporting Information Figure 1b). Biotite with low Mg# (48 mol%), calcic amphibole classified as Fe-pargasite or hastingsite (Leake et al., 2004), accessory hematite, Ti-oxides, and zircon (Supporting Information Table 3) were also observed.

Group 2 (Figure 4e), constituted by pitchers CM 17, CM 18 and CM 25, kettle CM 21, and cooking pot CM 20 (Table 2), was characterized by light brown, red, or reddish brown pastes, often zoned. The temper was composed of predominant volcanic (CM 17, CM 18, CM 25) or siliciclastic (CM 20, CM 21) grains. Rare calcite grains, partially or completely decomposed, were also observed for this group of samples. Crystals or polycrystalline aggregates of quartz and arenaceous fragments represented the siliciclastic grains (Figure 4f), while the volcanic phases were represented by K-feldspar ($\text{An}_0\text{Ab}_{4-36}\text{Or}_{96-64}$), lower bytownite ($\text{An}_{85}\text{Ab}_{13}\text{Or}_2$) (Supporting Information Figure 1a and Table 1), diopside and Fe-rich diopside (Supporting Information Figure 1b and Table 2), biotite, hastingsite (Supporting Information Table 3), and trachytic scoriae. Leucite (Figure 4g; Supporting Information Table 3) and Lc-bearing scoriae only occurred in sample CM 25, while traces of garnet were identified in sample CM 21 (Table 2). The aplastic inclusions (packing 10–25%), moderately sorted (average $\sigma_{\phi=0.74}$), with a subcircular shape (average C = 0.81) and dimensions ranging from very fine granules (2.01 mm) to fine silt (0.01 mm; average $\phi_{\text{mF}} = 4.9$), were arranged in a bimodal texture, as testified by the negative tails of the ϕ size curves toward low values (Figure 4h). The coarser particles, most probably representing the temper as also inferred by their textural features characterized by well-rounded and well-sorted sandy-silty elements, appear compositionally consistent with Pleistocene beach sands (Balassone et al., 2016; Morra et al., 2013).

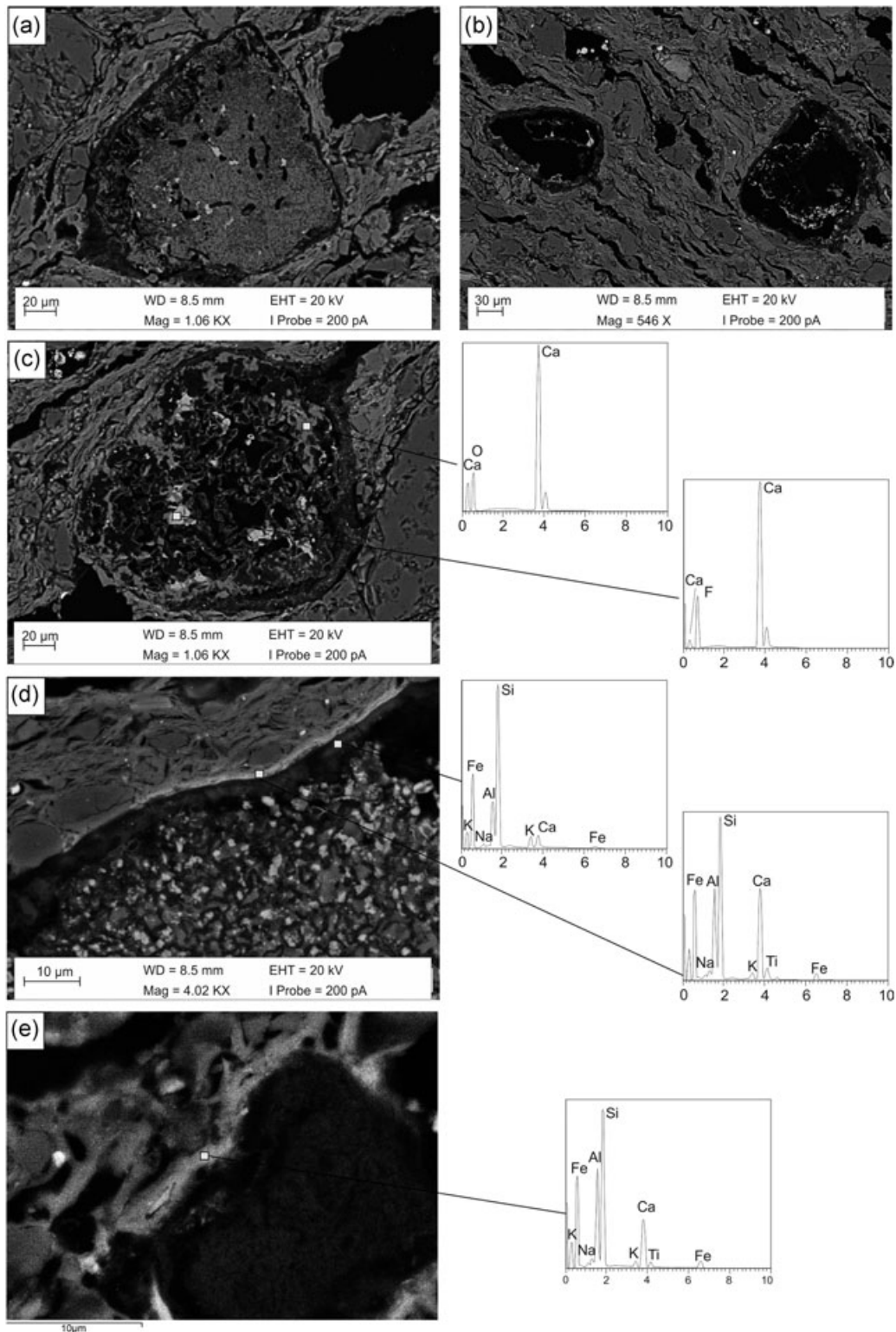


FIGURE 5 SEM/EDS results: (a) Electron backscattered micrograph of a partially decomposed carbonate grain; (b) Calcite ghosts; (c) Electron-backscattered micrograph and EDS microanalyses of a carbonate grain containing calcite and fluorite crystals. (d) Electron-backscattered micrograph and EDS microanalyses of the brighter and darker portions of the reaction rim developed around the carbonate temper grains. (e) Electron-backscattered micrograph and EDS microanalyses of the reaction rims developed around the calcite grains in the matrix of the calcareous sample CM 19. EDS: energy-dispersive X-ray spectroscopy; SEM: Scanning electron microscopy

XRF chemical analyses performed on the ceramic samples revealed that both Groups 1 and 2 had a similar composition, and most elements (SiO_2 , Al_2O_3 , Fe_2O_3 , MgO , Na_2O , K_2O , Rb , Zr , and Nb) varied in a very narrow range (Table 3). Similar concentrations of major oxides and especially of trace elements (e.g., Rb , Zr , and Nb) suggested that the exploited base clay could have been the same.

It is worth noting that the Group 1 samples show a slightly higher average concentration of calcium oxide (3.4 wt.%) when compared to Group 2 (average CaO = 1.5 wt.%), the latter characterized by higher average concentration of Al_2O_3 , Fe_2O_3 , and Zr (Figure 6; Table 3). The slight variations observed in the CaO contents could be due to the different abundance of carbonate temper added to the pastes, which is higher in Group 1.

Finally, the painted pitchers, CM 19 and CM 24, represented two outliers, being significantly different from the other samples. Sample CM 24 showed a fine-grained texture (0.01–0.10 mm; average ϕ_{mF} = 5.3) with a serial distribution of the residual aplastic grains, constituted by quartz, feldspar, and calcite (Figure 4h). In contrast, the pitcher, CM 19, presented a coarser paste due to the addition of volcanic temper (10–15%; Figure 4j). The aplastic particles were arranged in a bimodal texture and their dimensions varied from coarse sand (0.60 mm) to fine silt (0.01 mm; average ϕ_{mF} = 4.7), moderately sorted ($\sigma_{\phi=0.81}$) (Table 2). The temper was composed of K-feldspar ($\text{An}_0\text{Ab}_4\text{Or}_{96}$), plagioclase ($\text{An}_9\text{Ab}_{89}\text{Or}_2$) (Supporting Information Figure 1a and Table 1), diopside and Fe-rich diopside (Supporting Information Figure 1b and Table 2), abundant trachytic scoriae, minor Mg-rich olivine (Supporting Information Table 3), biotite, volcanic glass fragments and accessory Fe and Ti-oxides.

Despite textural differences, the chemical analyses highlighted a similar composition between samples CM 19 and CM 24 that was considerably different from groups 1 and 2. In fact, both pitchers were characterized by medium–high calcium oxide concentrations (9.1–14.3 wt.%), higher MgO (3.3–3.4 wt.%), and Sr (297–360 ppm) contents, as well as lower SiO_2 (57.7–59.0 wt.%; Figure 5a), Zr (151–221 ppm), and Nb (18–26 ppm; Figure 5, Table 3).

7 | PROVENANCE DETERMINATION OF CERAMICS

One of the main archaeological goals of this study was to establish the provenance of the Aegean-like pottery, widely imitated in southern Italy workshops (Gliozzo et al., 2005a). Thus, the textural, mineralogical, and petrographic features of the ceramic pastes were compared with the available data of similar pottery recovered in other archaeological contexts. The comparison was carried out with imports produced in the Aegean islands, the Attica region, and western Asia Minor (Istenič & Schneider, 2000) and discovered in the archaeological sites of Roma (Whitehouse, Barker, Reece, & Reese, 1982), Ostia (Predieri & Sfrecola, 2000), San Giacomo degli Schiavoni (Albarella et al., 1993), Aquileia (Italy; Ceazzi & Del Brusco, 2014; Istenič & Schneider, 2000), and Emona (Slovenia; Istenič & Schneider, 2000).

TABLE 3 Chemical composition of analyzed pottery by X-ray fluorescence, in terms of major oxides (wt.% recalculated to 100% on a loss on ignition-free basis) and trace elements (parts per million)

Sample	SiO_2	TiO_2	Al_2O_3	Fe_2O_3	MnO	MgO	CaO	Na_2O	K_2O	P_2O_5	Rb	Sr	Y	Zr	Nb	Ba	Cr	Ni	Sc	
Group 1																				
CM 09	67.53	0.75	16.48	6.23	0.06	1.57	3.00	1.18	3.07	0.13	217.6	198.5	38.8	299.7	37.9	541.7	88.9	35.5	14.1	
CM 15	66.90	0.79	17.71	6.45	0.05	1.61	2.31	1.15	2.93	0.09	185.3	173.3	43.7	295.5	37.1	458.3	94.8	44.9	12.9	
CM 16	66.63	0.71	16.20	6.23	0.06	1.61	4.38	1.17	2.90	0.10	198.9	204.6	32.0	295.1	33.3	530.6	98.7	43.5	11.5	
CM 22	64.96	0.79	17.84	6.61	0.06	1.87	3.76	1.02	2.98	0.11	209.9	179.6	27.5	264.3	32.7	402.9	115.1	49.3	12.4	
CM 27	65.64	0.82	17.86	6.65	0.06	1.53	3.35	1.13	2.87	0.09	187.8	184.6	39.3	313.6	40.2	434.8	99.1	50.8	12.3	
average	66.33	0.77	17.22	6.44	0.06	1.64	3.36	1.13	2.95	0.10	199.9	188.1	36.3	293.6	36.2	473.7	99.3	44.8	12.6	
σ	1.03	0.04	0.81	0.20	0.00	0.13	0.78	0.06	0.08	0.02	13.91	13.08	6.44	18.04	3.18	60.47	9.73	6.01	0.96	
Group 2																				
CM 17	66.39	0.82	18.41	6.87	0.05	1.86	1.40	1.14	2.93	0.11	192.9	156.4	40.9	311.7	34.6	463.9	108.8	48.0	14.3	
CM 18	65.46	0.91	19.63	7.36	0.10	1.39	1.21	1.19	2.69	0.05	225.6	156.9	33.4	313.6	36.9	560.5	106.4	42.5	14.9	
CM 21	68.26	0.78	16.31	6.82	0.06	1.62	2.04	1.08	2.92	0.09	198.9	169.7	43.8	296.1	33.2	595.7	112.3	42.7	15.9	
CM 25	67.55	0.79	18.01	6.38	0.04	1.61	1.23	1.29	3.02	0.07	187.2	172.0	33.8	325.8	38.5	639.8	98.6	37.2	14.8	
average	66.92	0.83	18.09	6.86	0.06	1.62	1.47	1.18	2.89	0.08	201.2	163.8	38.0	311.8	35.8	565.0	106.5	42.6	15.0	
σ	1.24	0.06	1.37	0.40	0.03	0.19	0.39	0.09	0.14	0.03	16.99	8.25	5.19	12.19	2.36	74.79	5.81	4.41	0.67	
CM 19	59.02	0.77	16.02	6.68	0.12	3.44	9.05	1.31	3.36	0.23	183.0	359.8	38.7	221.1	25.9	512.5	114.2	54.9	15.8	
CM 24	57.68	0.70	14.00	5.83	0.08	3.32	14.31	0.79	3.01	0.27	149.4	297.4	28.9	150.9	18.4	297.1	133.5	70.2	16.5	
average	58.35	0.74	15.01	6.26	0.10	3.38	11.68	1.05	3.19	0.25	166.2	328.6	33.8	186.0	22.2	404.8	123.9	62.6	16.2	
σ	0.95	0.05	1.43	0.60	0.03	0.08	3.72	0.37	0.24	0.03	23.76	44.12	6.93	49.64	5.30	152.31	13.65	10.82	0.49	

Note. Average values and standard deviation (σ) for each petrographic group were also reported.

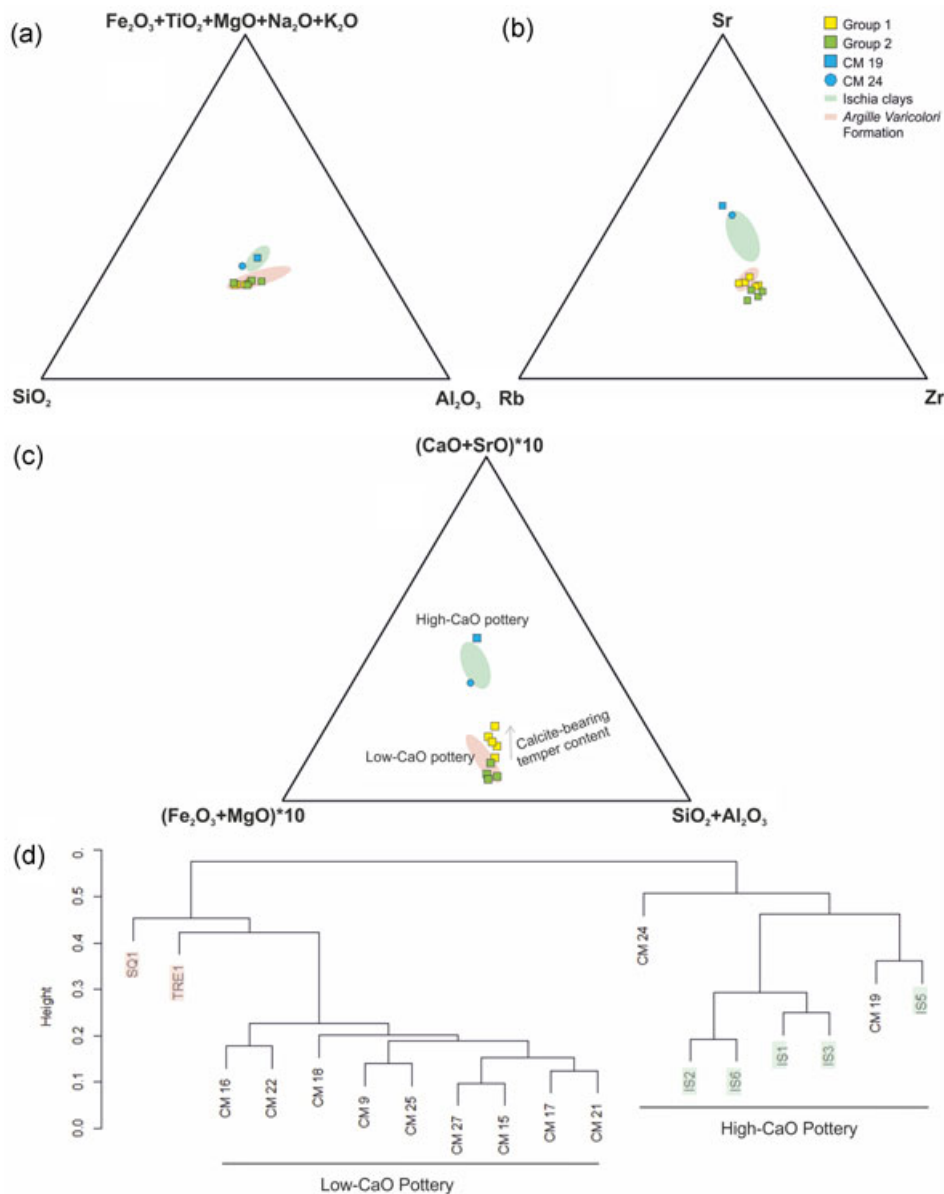


FIGURE 6 Ternary diagrams representative of major oxides (a,c) and trace element (b) concentrations. Hierarchical cluster analysis dendrogram (d) resulting from multivariate statistical analyses of chemical data. Clays from the Island of Ischia (IS 1, 2, 3, 5, 6) and the *Argille Varicolori* Formation (SQ1, TRE1; data from De Bonis et al., 2013) were also reported for comparison [Color figure can be viewed at [wileyonlinelibrary.com](https://onlinelibrary.wiley.com)]

Although the available archaeometric data mostly referred to thin sections and scant chemical analyses, the pottery samples from Cuma appeared quite dissimilar. Indeed, ceramic products from the Aegean islands and Attica region were characterized by coarse fabrics containing crystalline schist or metamorphic granules (Istenič & Schneider, 2000; Predieri & Sfrecola, 2000) whereas products from western Asia Minor (region of Phocaea) showed a chemical (e.g., higher Zr and Al_2O_3 bulk content) and mineralogical composition (e.g., acidic volcanic rocks and abundant fragments of pumice; Istenič & Schneider, 2000) that differs from those of the Cuman pots. In addition, the comparison with the imitations recovered in Central Italy (Predieri & Sfrecola, 2000) and in the Apulian workshop of San Giusto (Gliozzo et al., 2005a; Gliozzo, Turchian, Memmi Tubanti, Fortina, & Volpe, 2005b) also highlighted

considerable differences (e.g., calcareous pastes with volcanic temper) that excluded importation from those extraregional contexts.

A comparison with published data failed to find a match for the fabrics of the Aegean-like pottery from Cuma. Hence, we explored the hypothesis of a local or microregional workshop that imitated the imported ceramic shapes by comparing the composition of the base clay and the mineral chemistry of the temper grains with raw materials outcropping in the Campania region (Germinario, 2015; Germinario et al., 2018; Grifa, Langella, Morra, & Soricelli, 2005; Grifa, Morra, Langella, & Munzi, 2009a; Grifa et al., 2015, 2013, 2016; Guarino et al., 2016, 2011; Morra et al., 2013). As previously observed, the chemical differences between Groups 1 and 2 and the two loners (CM 19, CM 24) clearly point to the utilization of different

base clays. A high-CaO base clay (HCC; De Bonis et al., 2013) was used for samples CM 19 and CM 24, whereas low-CaO clayey deposits (LCC; De Bonis et al., 2013) were used for all the other samples (Table 3). From the comparison with the Campanian clayey deposits that most probably supplied the ancient workshops (De Bonis et al., 2013), the composition of the high-CaO pitchers is consistent with the chemical features of Ischia clayey deposits (De Bonis et al., 2013; Figure 6a,b,c), largely adopted in Campanian ceramic productions from the Greek to Medieval periods (De Bonis et al., 2013, 2016; Grifa et al., 2009a).

With regard to the low-CaO ceramics (Groups 1 and 2), the samples displayed good compositional similarities with the basinal clays of the *Argille Varicolori* Formation, also exposed in the inland areas of the northern Campania region, in the Caserta province (De Bonis et al., 2013; Figure 6a,b,c). According to De Bonis et al. (2013), the *Argille Varicolori* sediments are characterized by a polymineral association of clay minerals (kaolinite, illite, and an illite-smectite mixed-layer with a strong smectitic component) typical of pottery clays (Konta, 1995). These hypotheses are supported by the statistical treatment of the data (PCA and HCA), carried out omitting MnO, P₂O₅, and Ba, easily prone to post-depositional contamination (see below). Calcium oxide was also omitted due to the fact that the occurrence of carbonate-bearing temper could influence the statistical results.

The resulting dendrogram confirms the compositional affinities among Groups 1 and 2 and the *Argille Varicolori* deposits (SQ1, TRE1; De Bonis et al., 2013) that form a homogeneous group on the left side of the diagram (Figure 6d). The loners, pitchers CM 19 and CM 24, instead, were clustered on one side of dendrogram along with the Ischia clays (IS 1, 2, 3, 5, 6; De Bonis et al., 2013; Figure 6d), inferring a local production of the ceramic finds, and confirmed by the chemical analyses of the temper grains.

Further proof of a local production also derives from the analyses of the temper grains. It is widely acknowledged, in fact, that the mineralogy and mineral chemistry of temper grains can be a valuable tool for the provenance identification of pottery (Maggetti, 2001). For this reason, the mineralogical and textural features of the temper grains contained in the ceramic body were compared with the beach sands in the Cuma region. The Campanian littoral is characterized by a complex sedimentary system that influences its mineralogy. Apennine siliciclastic and carbonate outcrops widely affect the mineralogical assemblage of sands, although the occurrence of a secondary volcanic component from the activity of volcanic systems (Somma-Vesuvius, Phlegraean Fields, and Roccamonfina) is common (Balassone et al., 2016; Morra et al., 2013). These three main mineralogical components vary in concentration moving north to south along the coast (Balassone et al., 2016).

The occurrence of a mixed carbonate + volcanic + siliciclastic temper in Group 1 permitted locating the supply zone of temper grains just north of Cuma where this type of beach sand is supplied by the actions of the Volturno River (Balassone et al., 2016). Moreover, the mineral chemistry of the volcanic fraction was compatible with minerals forming the Phlegraean volcanics (Morra

et al., 2013). Microscopic and mineralogical data highlighted that the amount of carbonate component decreases in the Group 2 samples and sample CM19, whereas, a volcanic component matching the mineralogical composition of Phlegraean Fields rocks occurs (e.g., sanidine, diopside, Fe-rich diopside, biotite; Grifa et al., 2009a), suggesting a supply of raw materials close to the ancient Cuma shoreline (Balassone et al., 2016; Morra et al., 2013). Hence, the aforementioned arguments lead to the hypothesis that ancient Cuma (or the surrounding area) contained a workshop producing local common wares and imitation Aegean-like shapes.

8 | ESTIMATED FIRING TEMPERATURES

The firing conditions and temperatures experienced by the pottery were estimated by the detection of the “firing markers” that differ in calcareous and noncalcareous pastes. With regard to the HCC, the newly formed Ca-silicates (e.g., gehlenite, diopside, anorthite) can be considered as thermal indicators for the estimation of firing temperatures achieved by the ceramic pastes. It is widely accepted that when firing temperatures are increased, calcite in base clays reacts with the Si- and Al-rich phases to form Ca-silicates, starting from approximately 850°C (Cultrone et al., 2001; De Bonis, Cultrone, Grifa, Langella, & Morra, 2014; Grifa et al., 2009b).

In the case of the painted pitcher CM 19, the SEM observations show that tiny calcite grains (ranging in size from 15 to 20 μm) display thin Ca-silicates reaction rims (Figure 5e), thus inferring the occurrence of an interaction between the calcium oxide and the clayey matrix. However, the firing temperatures and/or the soaking time were probably not sufficient to form an XRPD-detectable amount of newly formed Ca-silicates (Table 4). The occurrence of a residual calcite (ca. 4%; Table 5) measured by thermogravimetric-differential scanning calorimetric analyses permits estimating a firing temperature ranging from 800 to 850°C, in agreement with Grifa et al. (2009b) and De Bonis et al. (2014).

Conversely, in low-CaO clayey materials, firing markers are only barely distinguishable. The increase of firing temperatures produced the gradual breakdown of clay minerals with the exception of some

TABLE 4 Mineralogical composition (X-ray powder diffraction) of ceramic samples

	Samples	Qz	Fsp	Ill/mica	Cpx	Cal	Hem
Group 1	CM 09	xxxx	xx	tr	–	x	x
	CM 16	xxxx	xx	tr	–	xx	tr
	CM 27	xxxx	xx	xx	–	xx	tr
Group 2	CM 18	xxxx	xx	–	–	–	x
	CM 20	xxxx	xx	xx	–	–	–
	CM 21	xxxx	xx	–	tr	–	xx
	CM 25	xxxx	xx	x	x	–	tr
	CM 19	xxxx	xxx	xx	x	xx	x

Abbreviations (Whitney & Evans, 2010): Cal: calcite; Ill: illite; Cpx: clinopyroxene; Fsp: feldspar; Hem: hematite; Qz: quartz. xxxx = predominant, xxx = abundant, xx = frequent, x = sporadic, tr = traces

TABLE 5 Weight-loss and enthalpy changes of ceramic samples by thermogravimetric-differential scanning calorimetric analyses

Sample	40–150°C				150–600°C				600–800°C				800–1,150°C				LOI (wt%)
	ΔW (%)	DSC ^a (°C)	DTG (°C)	DTG (°C)	ΔW (%)	DSC ^{a,b} (°C)	DTG (°C)	DTG (°C)	ΔW (%)	DSC ^a (°C)	DTG (°C)	DTG (°C)	ΔW (%)	DSC ^b (°C)	DTG (°C)		
Group 1																	
CM 09	0.1	-	112	112	1.0	478 ^b	268	644	0.6	572–655	644	644	0.3	1,063	1,017–1,103	2.0	
CM 16	0.4	79	112	291	1.5	480 ^b	291	676	1.6	572–685	676	676	0.3	846–1,073	1,037–1,125	3.8	
CM 27	0.3	74	117	442	1.8	460 ^b	442	675	1.4	684	675	675	0.3	988	1,121	3.8	
Group 2																	
CM 17	0.2	-	-	218	1.5	473 ^b	218	598	0.2	573	598	598	0.2	1,029	1,022	2.0	
CM 18	0.3	-	110	-	1.3	246 ^a	-	-	0.1	574	-	-	0.1	1,049	-	1.8	
CM 20	0.9	73	122	440	2.6	-	440	640–774	1.0	-	640–774	640–774	0.7	987	1,019–1,119	5.2	
CM 21	0.1	-	101	390	1.4	409 ^a –486 ^b	390	630	0.4	576	630	630	0.1	1,017	-	1.9	
CM 25	0.1	-	109	232	0.9	466 ^b	232	-	0.1	574	-	-	0.1	1,026	-	1.1	
CM 19	0.4	92	116	-	1.3	-	-	675	1.9	573–690	675	675	0.5	1,067	1,119	4.0	

Note. Negative peaks observed on derivative thermogravimetric curves are also reported ^aendothermic peak; ^bexothermic peak. ΔW: weight loss (by thermogravimetric); DSC: differential scanning calorimetry; DTG: derivative thermogravimetric curve; LOI: loss on ignition.

phyllosilicates (e.g., illite/mica) that persist in the dehydroxylated form up to ca. 950°C (Cultrone et al., 2001); the only newly formed mineral was hematite that begins developing at around 700°C (Nodari, Marcuz, Maritan, Mazzoli, & Russo, 2007).

The equivalent firing temperatures reported here are based on the presence of residual illite/mica and hematite on the XRPD pattern. Firing temperatures of ca. 800°C were estimated for samples CM 27 and CM 20, where illite/mica still occurred along with very low amounts of hematite (Table 4). Higher firing temperatures (ranging from 850 and 900°C) were hypothesized for the ceramic samples in which hematite was present in higher amounts (CM 09, CM 16, CM 25) and illite/mica only occurred in traces (Table 4). Finally, samples CM 18 and CM 21, characterized by the highest amount of hematite and by the lack of illite (Table 4), were most probably fired at the highest temperatures (950°C).

9 | POST-DEPOSITIONAL PHENOMENA

As previously described, the ceramic samples experienced a long burial in an environment that enhanced post-depositional alteration, and whose effects were clearly recognizable by TG analyses in the 250 and 500°C thermal range. The FTIR spectra of the EGA, in fact, recorded a sharp emission of CO₂, often followed by the emission of SO₂ (Figure 7), the latter characterized by an exothermic effect at ca. 475°C (Table 5). The release of carbon dioxide should be attributed to the combustion of organic matter, most probably deposited on the ceramic artifacts during their burial (Bayazit, Işık, Issi, & Genç, 2014; Ravisankar, Naseerutheen, Rajalakshmi, Raja Annamalai, & Chandrasekaran, 2014; Shoal, 1994). Although incompletely combusted organic matter in clays can occur in the fired cores of pottery, several clues suggest a secondary origin of the organic material recovered in our analysis. The post-depositional conditions suffered by the vessels, as well as the absence of both a sharp zonation of the ceramic body (e.g., sandwich structure) and mineralogical phases (e.g., spinel, hercynite) that generally form during the firing of clays containing organic matter (Maritan, Nodari, Mazzoli, Milano, & Russo, 2006 and reference therein), support this hypothesis. In contrast, the emission of sulphur dioxide can be ascribed to the occurrence of pyrite, widely observed in the pores and fissures of the ceramic pastes (Figure 8) which decomposes at temperatures between 450 and 500°C, forming hematite and releasing SO₂ (Hammack, 1987; Hammack, Lai, & Diehl, 1988).

Spherical aggregates of equigranular tiny pyrite crystals (“pyrite framboids”; Sawlowicz, 1993) were recognized by SEM observations (Figure 8). Disseminated euhedral pyrite crystals were also observed, intimately mixed within framboids of similar size. Such a widespread occurrence of pyrite presumes the availability of iron and sulphur (of organic or inorganic origin) in an anoxic environment, in which the activity of sulphate-reducing bacteria was enhanced (Sawlowicz, 1993; Schoonen, 2004). The well, sealed by the funerary inscription, dug in a volcanic tuff, submerged by groundwater, and containing decomposing organic matter, could have represented an “ideal”

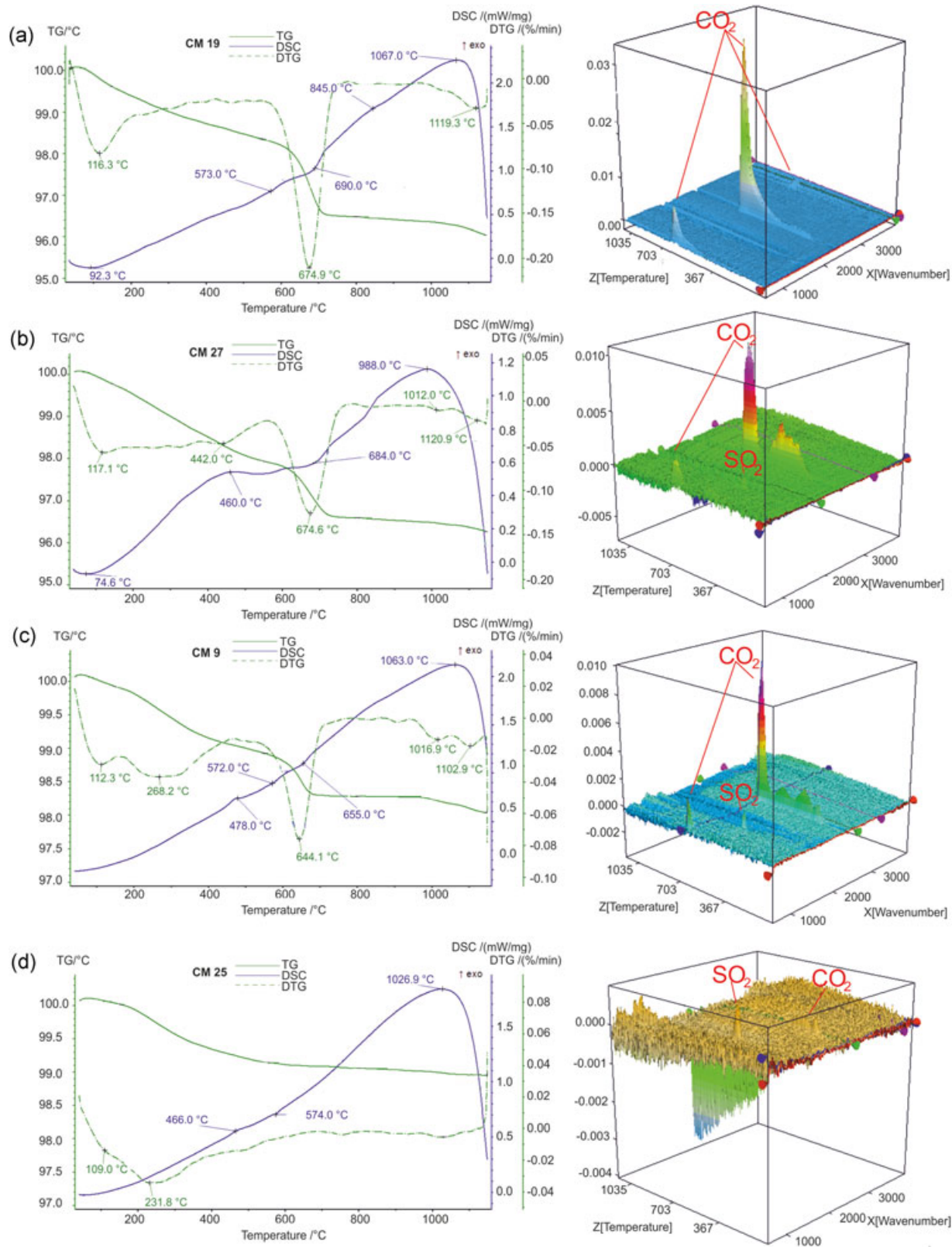


FIGURE 7 Thermogravimetric-differential scanning calorimetric curves (left column) and Fourier transform infrared spectra of evolved gases (right column) for samples CM 19 (a), CM 27 (b), CM 9 (c), and CM 25 (d) [Color figure can be viewed at wileyonlinelibrary.com]

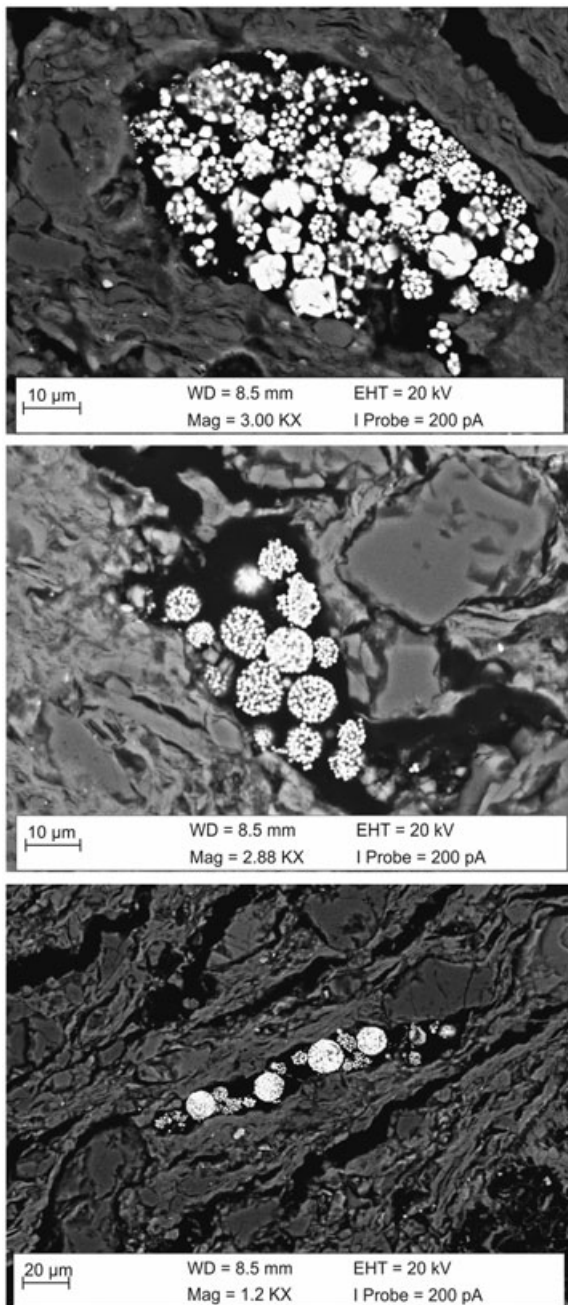


FIGURE 8 Pyrite framboids filling the pores of ceramic pastes

environment for the formation of the pyrite framboids observed in the ceramic samples, here preserved for a long period.

10 | CONCLUSIONS

Ancient Cuma is among the most important sites of prehistoric to Byzantine ceramic manufacturing in the Campania region, as highlighted by recent archaeological and archaeometric research. In addition to locally manufactured pottery, a large amount of imported ceramics had long circulated due to the proximity of important port hubs such as Puteoli and Misenum, particularly in the Roman period.

Thus, deciphering the provenance and technology of imported vessels could provide interesting scenarios on trade relationships with other areas of the Mediterranean coast, especially during the Late Roman period, when a large social and economic crisis affected Roman Empire territories, significantly reducing extraregional trade.

In this present research, vessels unearthed in a well associated with a Late Roman period workshop represent an exceptional closed context for examining some products assumed to have been imported on a typological basis. Numerous archaeologists have focused their attention on particular categories of pottery, namely “corrugated cooking pots,” similar to artifacts produced in Eastern Mediterranean areas and widely imitated in Southern Italy, and pyriform pitchers, recorded for the first time in an Italian archaeological context. Moreover, samples of painted pitchers were also investigated, to confirm the local production of such vessels, also attested in other regional contexts.

Our archaeometric analyses highlighted the occurrence of three different fabrics that cut across the ceramic classes (table or cooking ware). The painted pitchers were made with high-CaO clays (average CaO = 12 wt.%), often tempered with volcanic sands. A local production was inferred for this type of pottery due to the mineralogical, textural, and chemical features of the clay bodies as well as the mineral chemistry of the volcanic temper that shows quite good compositional affinities with Phlegraean volcanics. In addition, the chemical composition of the ceramic vessels suggests the exploitation of Ischia clayey raw materials as largely debated and argued for other local pottery manufacturing (De Bonis et al., 2013, 2016; Grifa et al., 2009a; Olcese, 2010, 2012, 2017).

Regarding the presumed exotic types, namely the Aegean-like cooking pots and the pyriform pitchers, the analytical results highlighted that typological differences also reflected the exploitation of different raw materials with respect to the painted pitchers. In fact, these vessels were crafted using a low-calcium base clay (CaO content ≤ 4 wt.%), displaying compositional similarities with basinal clays available in the inland areas of the northern Campania region, along with mixed-source temper grains, composed of carbonates, siliciclastic and volcanic phases.

Today, based on our current knowledge, the occurrence of such carbonate-rich temper has never been reported in ceramic productions from Cuma. On the contrary, the large data set of archaeological and archaeometric data of pottery revealed an enduring tradition in volcanic temper exploitation (Greco et al., 2014; Grifa et al., 2009a; Morra et al., 2013; Munzi et al., 2014). Taking into consideration the textural features (sorting and circularity) and the mineralogical assemblage, such a mixed-source temper resembled the shoreline deposits from Mondragone to north of Cuma, where beach sands are affected by the flux of siliciclastic and carbonate sediments of the Volturno River with a volcanic component derived from Campanian volcanoes (Balassone et al., 2016; Morra et al., 2013). It is worth highlighting that such sand was a valuable geomaterial, largely used in antiquity by Phlegraean artisans (including Cuma) as starting materials for glass and green/blue pigments, as also claimed by Vitruvius (Grifa et al., 2016). Hence, the cooking pots of presumed Aegean-like tradition can be considered as imitations since the

artifacts from the Eastern Mediterranean pottery tradition are sensibly different as characterized by the occurrence of metamorphic or acidic volcanic-tempered pastes (Istenič & Schneider, 2000); moreover, they also differ from other Italian imitations, in which a calcareous paste plus volcanic temper was recognized (Gliozzo et al., 2005a).

With regard to the pyriform pitchers, unfortunately no stylistic comparison can be found in other Mediterranean contexts; nevertheless, they strictly match mineralogical, textural, and chemical features of Aegean-like cooking pots. This could be reasonably framed in the social and historical context of late third century A.D. in this area, when, despite the beginning of the severe economic and political crisis that later affected the Western Roman Empire, commercial trade in the Mediterranean Sea was still quite active. The evidence of this circulation of goods, styles and ideas is highlighted by the imitation of Aegean common wares in different contexts of Southern Italy; it is likely that the artisans responded to a market requirement that favored the imitation of more fashionable forms (with better performances?) than those sold in the high frequency system of markets, called *nundinae* (Grifa et al., 2015; Soricelli, 2001). In the meantime, the development of microregional production continued following its own tradition, and probably developed new types by exploiting several sources of geomaterials, as in the case of pyriform pitchers, here attested and studied for the first time.

ACKNOWLEDGMENTS

The authors thank all the research staff of Centre Jean Bérard for providing the ceramic artifacts and the Archaeological Superintendence of Campania for authorizing the archaeometric analyses. The authors warmly thank Professor Gianluca Soricelli for stimulating interesting discussions, and Professor Piergiulio Cappelletti for the XRPD analyses. The authors also thank Antonietta Luongo and Professor David Bish for revising the English form of the manuscript. This study was funded with “LEGGE REGIONALE 5/02 ANNUALITA’ 2008 Decreti Presidenziali N° 163 del 15.9.2010, N° 43 del 21.2.2011 e N° 97 del 27.4.2011” Campania Region grants (CG), the Sannio University Research Fund (FRA 2013, CG), and University Federico II of Naples Research Fund (FRA 2013, VM). The contribution of G. Cultrone was funded by the Spanish Government (Grant MAT2016–75889-R). Finally, the authors also thank the two anonymous reviewers and editors for their comments and suggestion that improved the former version of the manuscript.

ORCID

Celestino Grifa  <http://orcid.org/0000-0003-4723-8158>

REFERENCES

Albarella, U., Ceglia, V., & Roberts, P. (1993). S. Giacomo degli Schiavoni (Molise): An early fifth century AD deposit of pottery and animal bones from central Adriatic Italy. *Papers of the British School at Rome*, 61, 157–230.

- Arthur, P. (2007). Form, function and technology in pottery production from late antiquity to early middle ages. In L. Lavan, E. Zanini, & A. Sarantis (Eds.), *Late antiquity archaeology* (4, pp. 159–184). Boston: Brin, Leiden.
- Balassone, G., Aiello, G., Barra, D., Cappelletti, P., De Bonis, A., Donadio, C., ... Siciliano, A. (2016). Effects of anthropogenic activities in a Mediterranean coastland: The case study of the Falerno-Domitio littoral in Campania, Tyrrhenian Sea (southern Italy). *Marine Pollution Bulletin*, 112, 271–290.
- Barberi, F., Innocenti, F., Lirer, L., Munno, R., Pescatore, T., & Santacroce, R. (1978). The campanian ignimbrite: A major prehistoric eruption in the Neapolitan area (Italy). *Bulletin Volcanologique*, 41, 10–31.
- Bayazit, M., Işık, I., İssi, A., & Genç, E. (2014). Spectroscopic and thermal techniques for the characterization of the first millennium AD potteries from Kuriki-Turkey. *Ceramics International*, 40, 14769–14779.
- Bish, D. L., & Reynolds, R. C. J. (1989). Modern powder diffraction. In D. L. Bish, & J. E. Post (Eds.), *Reviews in mineralogy* (20, pp. 73–99). Chantilly: Mineralogical Society of America.
- Bonardi, G., Ciarcia, S., Di Nocera, S., Montano, F., & Sgrosso, I. (2009). Carta delle principali unità cinematiche dell’ Appennino meridionale. Nota illustrativa. *Lias Sources And Documents Relating To The Early Modern History Of Ideas*, 128, 47–60.
- De Bonis, A., Arienzo, I., D’Antonio, M., Franciosi, L., Germinario, C., Grifa, C., ... Morra, V. (2018). Sr-Nd isotopic fingerprinting as a tool for ceramic provenance: Its application on raw materials, ceramic replicas and ancient pottery. *Journal of Archaeological Science*, 94, 51–59.
- De Bonis, A., Cultrone, G., Grifa, C., Langella, A., & Morra, V. (2014). Clays from the Bay of Naples (Italy): New insight on ancient and traditional ceramics. *Journal of the European Ceramic Society*, 34, 3229–3244.
- De Bonis, A., Febraro, S., Germinario, C., Giampaola, D., Grifa, C., Guarino, V., ... Morra, V. (2016). Distinctive volcanic material for the production of Campana A ware: The workshop area of Neapolis at the Duomo Metro Station in Naples, Italy. *Geoarchaeology*, 31, 437–466.
- De Bonis, A., Grifa, C., Cultrone, G., De Vita, P., Langella, A., & Morra, V. (2013). Raw materials for archaeological pottery from the Campania region of Italy: A petrophysical characterization. *Geoarchaeology*, 28, 478–503.
- Borriello, G., Giglio, M., & Iavarone, S. (2016). Nuove evidenze sulla produzione di ceramica d’età romana in area flegrea: Uno scarico di fornace da Cuma (NA). *Rei Cretaria Acta*, 44, 9–18.
- Brun, J. P., & Munzi, P. (2010). La necropoli monumentale in età romana a nord della città di Cuma. In J. P. Brun (Ed.), *Cuma: Atti del quarantaquattresimo convegno di studi sulla Magna Grecia* (pp. 635–718). Taranto: Istituto per la storia e l’archeologia della Magna Grecia.
- Brun, J. P., & Munzi, P. (2011). Cumes (Italie). Les fouilles du centre jean-bérard 2000–2010. *Bulletin de la société française d’archéologie classique* (41, 2009–2010). *Revue Archéologique*, 5, 147–221.
- Brun, J. P., Munzi, P., & Botte, E. (2018). Cuma. Il monumento funerario della “Sfinge” (A63) nella necropoli della Porta mediana. In C. Capaldi (Ed.), *Complessi monumentali e arredo scultoreo nella Regio I Latium et Campania: Nuove scoperte e proposte di lettura in contesto, Atti del convegno internazionale, dicembre 2013* (pp. 121–148). Napoli: Quaderni del Centro Studi Magna Grecia.
- Carpenter, P., Counce, D., Kluk, E., & Nabelek, C. (2002). Characterization of corning EPMA standard glasses 951RV, 951RW, and 951RX. *Journal of Research of the National Institute of Standards and Technology*, 107, 703–718.
- Cavassa, L., Munzi, P., Brun, J. P., Botte, E., Germinario, C., Grifa, C., ... Morra, V. (2018). Cumes. Le matériel tardo-antique découvert dans un puits: Entre données typologiques et analyses archéométriques. In D. Dixneuf (Ed.), *LRCW 5-1 - Late roman coarse wares, cooking wares and amphorae in the Mediterranean: Archaeology and archaeometry* (pp. 385–405). Alexandria: Centre d’Études Alexandrines.
- Ceazzi, A., & Del Brusco, A. (2014). La ceramica comune, la ceramica da cucina locale e importata e le anfore dello scavo di via Bolivia, Aquileia

- (Udine-Italia. In N. Poulou-Papadimitriou, E. Noradou, & V. Kilikoglu (Eds.), *LRCW 4, Late roman coarse wares, cooking wares and amphorae in the mediterranean: Archaeology and archaeometry. The Mediterranean: A market without frontiers* (Vol. 1, pp. 943–953). Oxford: BAR International Series 2616 I, Archeopress.
- Cultrone, G., Rodriguez-Navarro, C., Sebastian, E., Cazalla, O., & De La Torre, M. J. (2001). Carbonate and silicate phase reactions during ceramic firing. *European Journal of Mineralogy*, 13, 621–634.
- Deino, A. L., Orsi, G., de Vita, S., & Piochi, M. (2004). The age of the Neapolitan yellow tuff caldera-forming eruption (Campi Flegrei caldera – Italy) assessed by ⁴⁰Ar/³⁹Ar dating method. *Journal of Volcanology and Geothermal Research*, 133, 157–170.
- Donovan, J. J., Hanchar, J. M., Picolli, P. M., Schrier, M. D., Boatner, L. A., & Jarosewich, E. (2002). Contamination in the rare-earth element orthophosphate reference samples. *Journal of Research of the National Institute of Standards and Technology*, 107, 693–701.
- Donovan, J. J., Hanchar, J. M., Picolli, P. M., Schrier, M. D., Boatner, L. A., & Jarosewich, E. (2003). A re-examination of the rare-earth-element orthophosphate standards in use for electron-microprobe analysis. *The Canadian Mineralogist*, 41, 221–232.
- Fabbi, B., Guarini, G., Arduino, E., & Coghé, M. (1994). Significato del fosforo nei reperti ceramici di scavo. In F. Burrigato, O. Grubbessi, & L. Lazzarini (Eds.), *Proceedings of the 1st European Workshop on Archaeological Ceramics* (pp. 183–192). Roma: Università degli Studi di Roma “La Sapienza”.
- Fedele, L., Scarpati, C., Lanphere, M., Melluso, L., Morra, V., Perrotta, A., & Ricci, G. (2008). The Breccia Museo formation, Campi Flegrei, southern Italy: Geochronology, chemostratigraphy and relationship with the Campanian Ignimbrite eruption. *Bulletin of Volcanology*, 70, 1189–1219.
- Germinario, C. (2015). *The Late Roman in Campania region. Socio-economic reconstructions through the mineralogical and petrographic study of ancient pottery* (Unpublished doctoral dissertation). Sannio University, Benevento.
- Germinario, C., Cultrone, G., De Bonis, A., Izzo, F., Langella, A., Mercurio, M., ... Grifa, C. (2018). The combined use of spectroscopic techniques for the characterisation of Late Roman common wares from Benevento (Italy). *Measurement*, 114, 515–525.
- Glozzo, E., Fortina, C., Turbanti, I. M., Turchiano, M., & Volpe, G. (2005a). Cooking and painted ware from San Giusto (Lucera, Foggia): The production cycle, from the supply of raw materials to the commercialization of products. *Archaeometry*, 47, 13–29.
- Glozzo, E., Turchiano, M., Memmi Tubanti, I., Fortina, C., & Volpe, G. (2005b). La produzione di ceramica da fuoco di San Giusto (Lucera, Foggia): Dall’approvvigionamento della materia prima alla commercializzazione del manufatto. In B. Fabbri, S. Gualtieri, & C. Volpe (Eds.), *Tecnologie di lavorazione e impieghi dei manufatti: Proceedings of the Congress “VII Giornata di Archeometria della ceramica* (pp. 47–70). Bari: Edipuglia.
- Greco, G., Tomeo, A., Ferrara, B., Guarino, V., De Bonis, A., & Morra, V. (2014). Cumae, the forum: Typological and archaeometric analysis of some pottery classes from sondages insight the temple with Portico. In G. Greco, & L. Cicala (Eds.), *Archaeometry, comparing experiences* (pp. 37–68). Pozzuoli: Quaderni del Centro Studi Magna Grecia.
- Grifa, C., De Bonis, A., Guarino, V., Petrone, C. M., Germinario, C., Mercurio, M., ... Morra, V. (2015). Thin walled pottery from Alife (Northern Campania, Italy). *Periodico di Mineralogia*, 84, 65–90.
- Grifa, C., De Bonis, A., Langella, A., Mercurio, M., Soricelli, G., & Morra, V. (2013). A Late Roman ceramic production from Pompeii. *Journal of Archaeological Science*, 40, 810–826.
- Grifa, C., Cavassa, L., De Bonis, A., Germinario, C., Guarino, V., Izzo, F., ... Morra, V. (2016). Beyond Vitruvius: New insight in the technology of Egyptian blue and green frits. *Journal of the American Ceramic Society*, 99, 3467–3475.
- Grifa, C., Cultrone, G., Langella, A., Mercurio, M., De Bonis, A., Sebastián, E., & Morra, V. (2009b). Ceramic replicas of archaeological artefacts in Benevento area (Italy): Petrophysical changes induced by different proportions of clays and temper. *Applied Clay Science*, 46, 231–240.
- Grifa, C., Langella, A., Morra, V., & Soricelli, G. (2005). Pantellerian ware from Miseno (Campi Flegrei, Napoli). *Periodico di Mineralogia*, 74, 69–86.
- Grifa, C., Morra, V., Langella, A., Cultrone, G., & Sebastián, E. (2006). Technological features of glazed Protomajolica ware from Benevento (Italy). In R. Fort, M. Alvarez De Buergo, M. Gomez-Heras, & C. Vazquez-Calvo (Eds.), *Heritage, weathering and conservation* (pp. 123–135). Amsterdam: Taylor & Francis.
- Grifa, C., Morra, V., Langella, A., & Munzi, P. (2009a). Byzantine ceramic production from Cuma (Campi Flegrei, Napoli). *Archaeometry*, 51, 75–94.
- Guarino, V., De Bonis, A., Faga, I., Giampaola, D., Grifa, C., Langella, A., ... Morra, V. (2016). Production and circulation of thin walled pottery from the Roman port of Neapolis, Campania (Italy). *Periodico di Mineralogia*, 85, 95–114.
- Guarino, V., De Bonis, A., Grifa, C., Langella, A., Morra, V., & Pedroni, L. (2011). Archaeometric study on terra sigillata from Cales (Italy). *Periodico di Mineralogia*, 80, 455–470.
- Hammack, R. W. (1987). *Evolved gas analysis – A new method for determining pyrite, bicarbonate and alkaline earth carbonates*. In Proceedings of the 8th WV Surface Mine Drainage Task Force Symposium. Morgantown, WV.
- Hammack, R. W., Lai, R. W., Diehl, J. R. (1988). Methods for determining fundamental chemical differences between iron disulfides and different geological provenances. Bureau of Mines Information Circular. Mine Water and Mine Waste. Pittsburgh, PA. 1, pp. 136–146.
- Istenič, J., & Schneider, G. (2000). Aegean cooking ware in the Eastern Adriatic. *Rei Cretaria Acta*, 36, 341–348.
- Izzo, F., Arizzi, A., Cappelletti, P., Cultrone, G., De Bonis, A., Germinario, C., ... Langella, A. (2016). The art of building in the Roman period (89 B.C. - 79 A.D.): Mortars, plasters and mosaic floors from ancient Stabiae (Naples, Italy). *Construction and Building Materials*, 117, 129–143.
- Jarosewich, E. (2002). Smithsonian microbeam standards. *Journal of Research of the National Institute of Standards and Technology*, 107, 681–685.
- Jarosewich, E., & Boatner, L. A. (1991). Rare-earth element reference samples for electron microprobe analysis. *Geostandards Newsletter*, 15, 397–399.
- Jarosewich, E., Gooley, R., & Husler, J. (1987). Chromium Augite – A new microprobe reference sample. *Geostandards Newsletter*, 11, 197–198.
- Jarosewich, E., & MacIntyre, I. G. (1983). Carbonate reference samples for electron microprobe and scanning electron microscope analyses. *Journal of Sedimentary Research*, 53, 677–678.
- Jarosewich, E., & White, J. S. (1987). Strontianite reference sample for electron microprobe and SEM analyses. *Journal of Sedimentary Research*, 57, 762–763.
- Konta, J. (1995). Clay and man: Clay raw materials in the service of man. *Applied Clay Science*, 10, 275–335.
- Langella, A., Bish, D. L., Cappelletti, P., Cerri, G., Colella, A., de Gennaro, R., ... de Gennaro, M. (2013). New insights into the mineralogical facies distribution of Campanian Ignimbrite, a relevant Italian industrial material. *Applied Clay Science*, 72, 55–73.
- Leake, B. E., Woolley, A. R., Birch, W. D., Burke, E. A. J., Ferraris, G., Grice, J. D., ... Whittaker, E. J. W. (2004). Nomenclature of amphiboles: Additions and revisions to the international mineralogical association’s amphibole nomenclature. *American Mineralogist*, 89, 883–887.
- Maggetti, M. (2001). Chemical analyses of ancient ceramics: What for? *Chimia*, 55, 923–930.
- Maritan, L., Nodari, L., Mazzoli, C., Milano, A., & Russo, U. (2006). Influence of firing conditions on ceramic products: Experimental study on clay rich in organic matter. *Applied Clay Science*, 31, 1–15.
- Morra, V., De Bonis, A., Grifa, C., Langella, A., Cavassa, L., & Piovesan, R. (2013). Minerog-petrographic study of cooking ware and Pompeian red

- ware (Rosso Pompeiano) from Cuma (Southern Italy). *Archaeometry*, 55, 852–879.
- Morra, V., Calcaterra, D., Cappelletti, P., Colella, A., Fedele, L., De' Gennaro, R., ... & De' Gennaro, M. (2010). Urban geology: Relationships between geological setting and architectural heritage of the Neapolitan area. *Journal of the virtual explorer*, 36, 3.
- Mukay, T., & Aoyagi, M. (2014). Un contexte de la fin du IIIe s. à Somma Vesuviana (Campanie, Italie). In N. Poulou-Papadimitriou, & E. V. Nodarou, (Eds.), *LRCW 4, late roman coarse wares, cooking wares and amphorae in the Mediterranean: Archaeology and archaeometry. The Mediterranean: A market without frontiers* (1, pp. 864–871). Oxford: BAR International Series 2616 I, Archeopress.
- Munzi, P., Guarino, V., De Bonis, A., Morra, V., Grifa, C., & Langella, A. (2014). The fourth century black-glaze ware from the northern periurban sanctuary of Cumae. In G. Greco, & L. Cicala (Eds.), *Archaeometry, comparing experiences* (pp. 69–87). Pozzuoli: Quaderni del Centro Studi Magna Grecia.
- Nodari, L., Marcuz, E., Maritan, L., Mazzoli, C., & Russo, U. (2007). Hematite nucleation and growth in the firing of carbonate-rich clay for pottery production. *Journal of the European Ceramic Society*, 27, 4665–4673.
- Olcese, G. (2010). Le anfore greco italiche: Archeologia e archeometria. In G. Olcese (Ed.), *Artigianato ed economia a Ischia e nel Golfo di Napoli* (p. 477). Roma: Edizioni Quasar.
- Olcese, G. (2012). *Atlante dei siti di produzione ceramica (Toscana, Lazio, Campania e Sicilia) con le tabelle dei principali relitti del Mediterraneo occidentale IV secolo a.C. - I secolo d.C.* Roma: Edizioni Quasar.
- Olcese, G. (2017). "PITHECUSAN WORKSHOPS" Il quartiere artigianale di S. Restituta di Lacco Ameno (Ischia) e i suoi reperti (p. 464). Roma: Edizioni Quasar.
- Orlando, P. (2014). Ceramiche comuni dal Rione Terra (Pozzuoli, Naples). *Rei Cretaria Acta*, 4, 451–460.
- Orsi, G., De Vita, S., & di Vito, M. (1996). The restless, resurgent Campi Flegrei nested caldera (Italy): Constraints on its evolution and configuration. *Journal of Volcanology and Geothermal Research*, 74, 179–214.
- Piomallo, M. (2004). Puteoli, il porto di Roma. In G. Zevi, & R. Turchetti (Eds.), *Le strutture dei porti e degli approdi antichi* (pp. 267–278). Soveria Manelli: Rubettino.
- Predieri, G., & Sfrecola, S. (2000). La ceramica comune di Ostia antica: Analisi minero-petrografiche. In C. Pavolini (Ed.), *La Scavi di Ostia XIII. La Ceramica Comune. Le forme in argilla depurata dell'Antiquarium* (pp. 45–65). Roma: Istituto Poligrafico e Zecca dello Stato.
- R Development Core Team (2008). *A language and environment for statistical computing*. Vienna, Austria: R Foundation for statistical Computing.
- Rathossi, C., & Pontikes, Y. (2010). Effect of firing temperature and atmosphere on ceramics made of NW Peloponnese clay sediments. Part I: Reaction paths, crystalline phases, microstructure and colour. *Journal of the European Ceramic Society*, 30, 1841–1851.
- Ravisankar, R., Naseerutheen, A., Rajalakshmi, A., Raja Annamalai, G., & Chandrasekaran, A. (2014). Application of thermogravimetry-differential thermal analysis (TG-DTA) technique to study the ancient potteries from Vellore dist, Tamilnadu, India. *Spectrochimica Acta - Part A: Molecular and Biomolecular Spectroscopy*, 129, 201–208.
- Rosi, M., Sbrana, A., & Principe, C. (1983). The Phlegraean fields: Structural evolution, volcanic history and eruptive mechanisms. *Journal of Volcanology and Geothermal Research*, 17, 273–288.
- De Rossi, G. (2002). Il porto di miseno tra costantino e gregorio magno: Nuova luce dalle recenti acquisizioni. In M. Khanoussi, P. Ruggeri, & C. Vismara (Eds.), *L'Africa Romana. Lo spazio marittimo del Mediterraneo occidentale: Geografia storica ed economia* (pp. 833–843). Roma: Carrocci.
- Sawlowicz, Z. (1993). Pyrite framboids and their development. *Geol. Rundschau*, 82, 148–156.
- Schoonen, M. A. A. (2004). Mechanisms of sedimentary pyrite formation. In J. P. Amend, K. J. Edwards, & L. T.W., (Eds.), *Sulfur biogeochemistry - past and present* (Vol. 379, pp. 117–134). Boulder: Geological Society of America.
- Shoval, S. (1994). The firing temperature of a Persian-period pottery kiln at Tel Michal, Israel, estimated from the composition of its pottery. *Journal of Thermal Analysis*, 42, 175–185.
- Soricelli, G. (2001). La regione vesuviana tra secondo e sesto secolo d.C. In E. Lo Cascio, & A. Storchi Marino, (Eds.), *Modalità insediative e strutture agrarie nell'Italia meridionale in età romana* (pp. 455–472). Bari: Edipuglia.
- Vicenzi, E. P., Eggins, S., Logan, A., & Wysoczanski, R. (2002). Microbeam characterization of corning archeological reference glasses: New additions to the Smithsonian microbeam standard collection. *Journal of Research of the National Institute of Standards and Technology*, 107, 719–727.
- Whitehouse, D., Barker, G., Reece, R., & Reese, D. (1982). The Schola Praeconum I: The coins, pottery, lamps and fauna. *Papers of the British School at Rome*, 50, 53–101.
- Whitney, D. L., & Evans, B. W. (2010). Abbreviations for names of rock-forming minerals. *American Mineralogist*, 95, 185–187.
- Williams, D. F. (1990). The study of ancient ceramics: The contribution of the petrographic method. In T. Mannoni, & A. Molinari (Eds.), *Scienze in archeologia, quaderni del dipartimento di archeologia e storia delle arti, università di siena* (pp. 43–64). Firenze: Edizione all'insegna del Giglio.

SUPPORTING INFORMATION

Additional supporting information may be found online in the Supporting Information section at the end of the article.

How to cite this article: Germinario C, Cultrone G, Cavassa L, et al. Local production and imitations of Late Roman pottery from a well in the Roman necropolis of Cuma in Naples, Italy. *Geoarchaeology*. 2019;34:62–79.
<https://doi.org/10.1002/geo.21703>